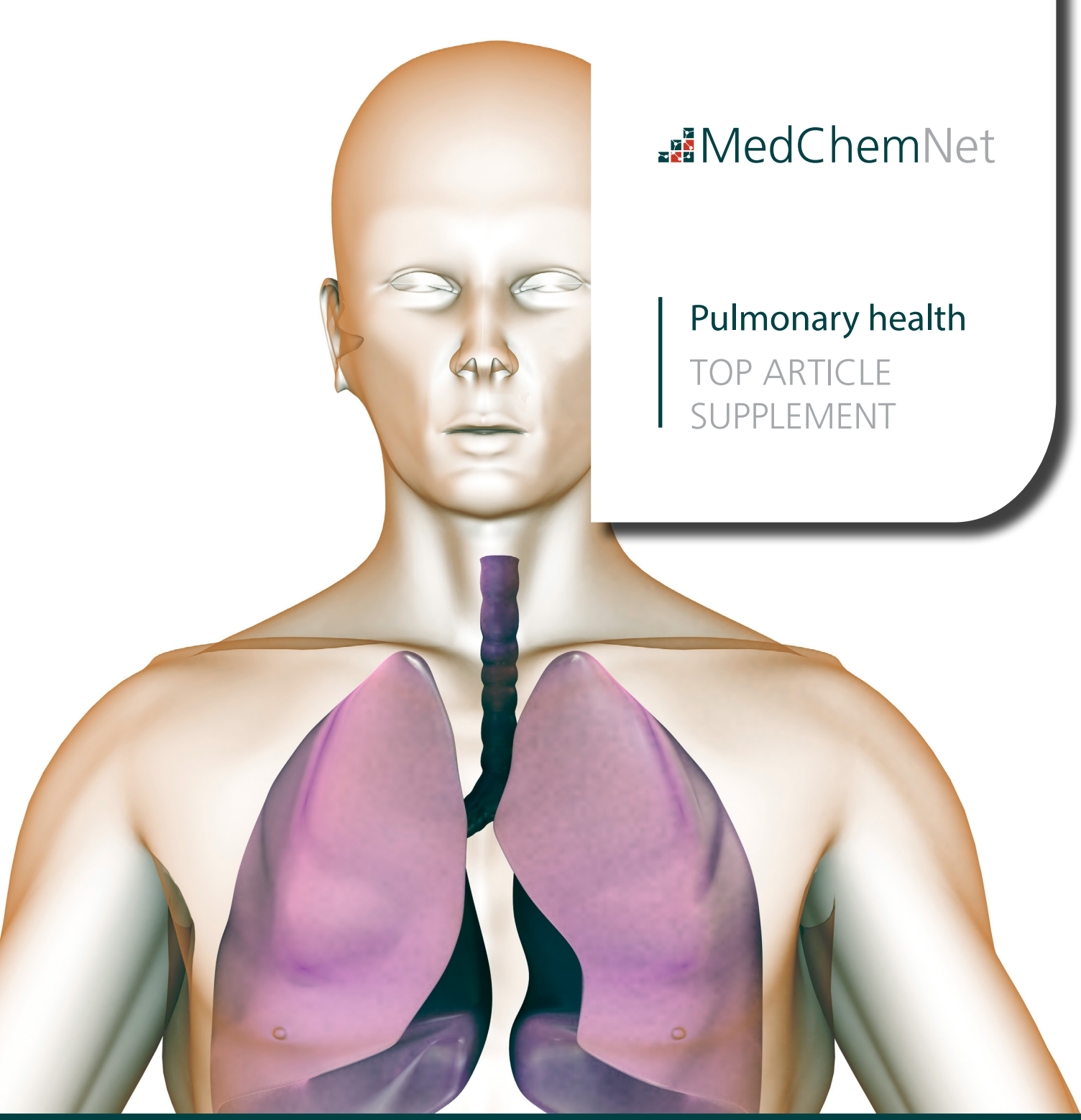

MedChemNet

Pulmonary health

TOP ARTICLE SUPPLEMENT

CONTENTS

fsg CONNECT

Special Report

For reprint orders, please contact: reprints@futuremedicine.com

Therapeutic Delivery

Nebulized drug delivery in respiratory medicine: what does the future hold?

John N Pritchard
[1]Respironics Respiratory Drug Delivery (UK) Ltd, a business of Philips Electronics UK Limited, Chichester, West Sussex, UK
john.pritchard@philips.com

In the later half of the 20th century, nebulized therapy was in decline, but in the 21st century the prospects for the expanded use of nebulized therapy within respiratory medicine look bright. The advent of mesh nebulizers, which combine the universal applicability of the nebulizer in the treatment of all respiratory patients with the convenience of portable inhaler use, is ideally timed to capitalize on the forecast of increased numbers of patients who will require nebulized therapy in the future. This special report will highlight some of the opportunities that the development of mesh nebulizers presents in the field of respiratory medicine.

First draft submitted: 27 January 2017; Accepted for publication: 3 April 2017; Published online: 4 May 2017

Keywords: adherence • breath activation • ease of use • jet • mesh • nebulizer • technique

Nebulized therapy

The nebulizer is the oldest of the three main types of aerosol delivery device, having been in use for over 150 years [1]. During this time, other inhaler devices, such as pressurized metered dose inhalers (pMDIs) and dry powder inhalers (DPIs), have been developed that have improved upon aspects of use, such as portability, speed of delivery and noise during operation, and increasingly replaced the nebulizer in the domiciliary setting during the late 20th century. However, none of these devices has duplicated the universal applicability of the nebulizer in the treatment of all groups of patients. The key attribute of the nebulizer is the ability of patients to receive a dose of drug while breathing with their typical tidal breathing or indeed atypical breathing during an exacerbation. This attribute is especially important for the very old, very young and very sick, and explains the enduring role of the conventional nebulizer in the treatment of respiratory diseases. Indeed at the beginning of the 21st century, it has been estimated that the number of inhaled doses administered by nebulizer was increasing at a faster rate than the pMDI or DPI [2], and the delivery of doses via nebulizer now represents the largest segment of the market by value in China [3].

The potential for increased volume of nebulizer use depends on both the size of the patient population needing treatment and the relative suitability of nebulizer treatment over other forms of inhaled treatment for that particular disease and patient group. Nebulized therapy has an established place in the treatment of a wide range of respiratory diseases, such as cystic fibrosis, pulmonary hypertension, bronchiectasis and a range of other respiratory diseases, but the largest potential for increased use of nebulized therapy is in the most common respiratory diseases.

Asthma & chronic obstructive pulmonary disease

Asthma and chronic obstructive pulmonary disease (COPD) are the two most common respiratory diseases worldwide, but the distribution of patient profiles differs significantly between the two diseases. Asthma affects a wide range of age groups from children to the elderly, and although a greater number

FUTURE SCIENCE part of fsg

of people suffer from asthma compared with COPD, the proportion of asthma patients for whom a nebulizer would be the most suitable device is lower due to this wider spread of ages and overall health of this population. Once a patient is of an age that they are able to synchronize pMDI activation with inhalation, or achieve the flow required of a DPI then these devices are usually prescribed for day-to-day treatment of asthma until severity of disease, or lack of manual dexterity becomes an issue. In addition to the issues of portability, speed of delivery and noise during operation, administration of nebulized doses of aerosol are generally more expensive than via pMDI or DPI per dose, so if the unique attributes of the nebulizer are not required then an inhaler is prescribed. Therefore, nebulizer therapy is generally confined to the previously mentioned extremes of the very young, very old or very sick asthma patients. One example of the potential benefits of advanced nebulized therapy in the sickest asthma patients has been shown in patients with oral-steroid-dependent asthma [4].

In the treatment of COPD, the unique attributes of the nebulizer contribute value to the treatment of more of the predominant elderly patient population, and the selection of nebulized drug delivery over pMDI or DPI is more likely. COPD is a leading cause of disease or injury worldwide, and is usually brought about by long-term exposure of the lungs to irritants, such as cigarette smoke and air pollution. This explains why patients with COPD are typically elderly, with the incidence in the USA increasing by over a factor of 3 between the ages of 55–64 and 65–74 [5]. Coupled to this, global life expectancy rose by 5 years between 2000 and 2015, with females born in the USA in 2015 expected to live to 81.6 years of age [6]. Therefore, with increasing life expectancy, the prevalence of COPD in the population is expected to rise, for example, in the USA the total burden of COPD measured by disability-adjusted life years contributed by elderly patients is expected to increase from approximately 30 to 40% by 2030 [7].

In addition to these increases due to rising longevity in the West, increasing cigarette use in China will also contribute to the rise of COPD, which is projected to become the third leading cause of disease or injury in China by 2030 [8]. This, along with the fact that since the start of the century China has reformed its healthcare system, and is now providing greater access to inhaled therapy, combines to make even greater growth in nebulizer use likely. Most patients are first diagnosed and treated with nebulizers as out-patients in a hospital setting. As a consequence, nebulized treatment is already the most commonly prescribed treatment in secondary- and tertiary-level hospitals in China [9]. Consequently, the treatment of COPD in the West and China has the potential to result in a significant increase in the volume of nebulizer use worldwide.

The extensive use of nebulized therapy in the treatment of patients with COPD is unsurprising given the problems that elderly patients have with inhaler use [10–12]; in addition to the issues arising from the need to synchronize device activation with inhalation and to inhale in a specified manner, poor dexterity and hand muscle strength from arthritis or other comorbidities can also inhibit proper use of pMDI and DPI devices [13]. After discharge from hospital following an exacerbation, around 50% of patients in the USA can expect to be prescribed a nebulized treatment [14]. The nebulized treatments available to these patients consist mainly of a combination of short-acting β-agonist and muscarinic drugs, meaning they may find themselves obliged to take up to four treatments per day, with the consequent burden in terms of treatment time that this entails.

The disconnect between the requirement for and the availability of long-acting drugs in a dosage form most suited for delivery to patients with COPD represents a significant opportunity to improve the treatment options available for those with COPD. The reason for the dearth of available long-acting nebulized drugs probably has its basis in a combination of the lack of appeal of bringing a new drug to market in what was considered an outdated technology with a small share of the overall inhaled market and the commercial considerations of drug development, including limited remaining patent life on the drug [15]. However, both these reasons look set to be overturned with the advent of mesh nebulizers, which now offer high portability, almost silent operation and rapid treatment times, while still providing the advantages consequent with nebulized treatment.

Nebulizers in drug development

Even when conventional nebulizers were the only option available, they were still commonly used during the early stages of drug development as they provided an easy and fast way of getting the drug into early-stage clinical trials [16]. However, once the potential for therapeutic benefit was proved, the nebulized formulation would typically be dropped in favor of a pMDI or DPI development to carry the drug through approval and release to the mass market. Considering the time taken to get the new drug through the development pipeline, it was generally not considered to be cost-effective to then launch a nebulized version, bearing in mind the time required to re-run dose ranging and pivotal Phase III studies against the backdrop of the patent expiry timetable.

However, the advent of patient-friendly mesh nebulizers along with the need for modern nebulized therapies for COPD, may now provide the incentive to use an alternative approach. The new approach is focused on using a nebulized formulation to take the drug right through development and onto the market, with possible inhaler development after successful demonstration of safety and efficacy. This has been modeled as likely to improve the return on R&D investments for new drug development [15,17], and in the case of the development of long-acting β-agonist and long-acting muscarinic antagonist drugs, would meet a need that is likely to grow more pressing with the growth in patients with COPD. In fact, there are signs that some drug companies are now responding to this gap in therapy options with the development of nebulized long-acting muscarinic antagonist drugs [18,19]. In the future, triple combinations of nebulized long-acting β-agonist with long-acting muscarinic antagonist and inhaled corticosteroids will further increase the treatment options available to patients with COPD.

New nebulizer technology

Up until the early 1990s, the two classes of nebulizer available to patients for domiciliary use were the jet and ultrasonic nebulizer. Although ultrasonic nebulizers were an advance over jet nebulizers in terms of noise during operation, they suffered from a couple of significant drawbacks; they could not be used for the delivery of drugs formulated as suspensions or viscose drugs, such as antibiotics, and they heated the drugs during treatment, such that thermolabile drugs (e.g., proteins or peptides) could be damaged [20,21]. Jet nebulizers were thus the main type used by respiratory patients, but use was tethered to an alternating current power supply, involved a lot of noise during treatment and required careful cleaning of the nebulizer cup after use.

The arrival of the battery-operated mesh nebulizer is set to change the outlook for nebulized therapy. Mesh nebulizers are highly portable, virtually silent in operation and provide a rapid rate of aerosol delivery and low residual volumes. Although mesh nebulizers are capable of nebulizing most drug formulations on the market today, the viscosity and surface tension of the formulation can affect output rate. Mesh nebulizers can typically deliver formulations of surface tension in the range 35–75 mN/m with a range of viscosities (Figure 1) [22], although the range is not as wide as for jet nebulizers (1–6 Cp) [23].

There is also some debate regarding the resilience of mesh nebulizers to misuse and failure to follow cleaning instructions [24,25], but the adoption of robust cleaning protocols should minimize these risks [26]. Also, in a simulated ventilation setting, it has been observed that residual volume of one type of mesh nebulizer can vary [27], but this is likely to be device specific, for example, it has been shown that some nebulizers maintain consistency of dose delivery even when tilted 45° off vertical (Figure 2) [28]. As with any new technology introduced into an established market, there is an adoption period while the initial designs and technical aspects are refined, and users become accustomed to differences in use and care of the equipment compared with existing technology.

Jet nebulizers currently represent around three quarters of the nebulizer market, but the use of mesh nebulizers is forecast to grow a third faster than jet nebulizers in the next few years [29]. This is despite the fact that in general mesh nebulizers are currently more expensive to purchase than jet nebulizers. The price difference varies between brands, models and countries, and can also be influenced by the cost of consumables as well as the warranty life of the product. An indication of the acceptance of this technology is given by an examination of clinical trial registers, which shows that the number of clinical trials performed using mesh nebulizers is already greater than those using jet nebulizers. This is not surprising given the previously mentioned considerations for early-stage drug development, coupled with the properties of mesh nebulizers, such as accurate dose delivery, which are advantageous in the conduct of dose-ranging studies.

Mesh nebulizers are more convenient than jet nebulizers when used to deliver aerosol to ventilated patients, as mesh nebulizers do not introduce additional pressures or flows into the ventilator circuit [30], whereas jet nebulizers may require adjustments to accommodate the additional source of air. As a consequence, many common makes of ventilator incorporate the drive circuitry for these devices, allowing the nebulizer to be driven directly from the ventilator. Mesh nebulizers are also more efficient at delivering drug to the ventilated patient [31], and breath-activation can be synchronized with the ventilation cycle for maximum delivery efficiency [32]. Mesh nebulizer technology, such as the Aerogen Solo can be fitted to a wide variety of ventilation circuits, including noninvasive ventilation, continuous positive airway pressure and high-flow nasal therapy, for use in both the emergency room and at home, thus allowing a continuum of care with the same technology for these patients.

Ease of use

Established mesh nebulizer designs have been shown to offer increased ease of use and patient satisfaction over jet nebulizers [33]. Advances in technical aspects of the latest generation of mesh nebulizers can be expected to improve upon the ease of use for the

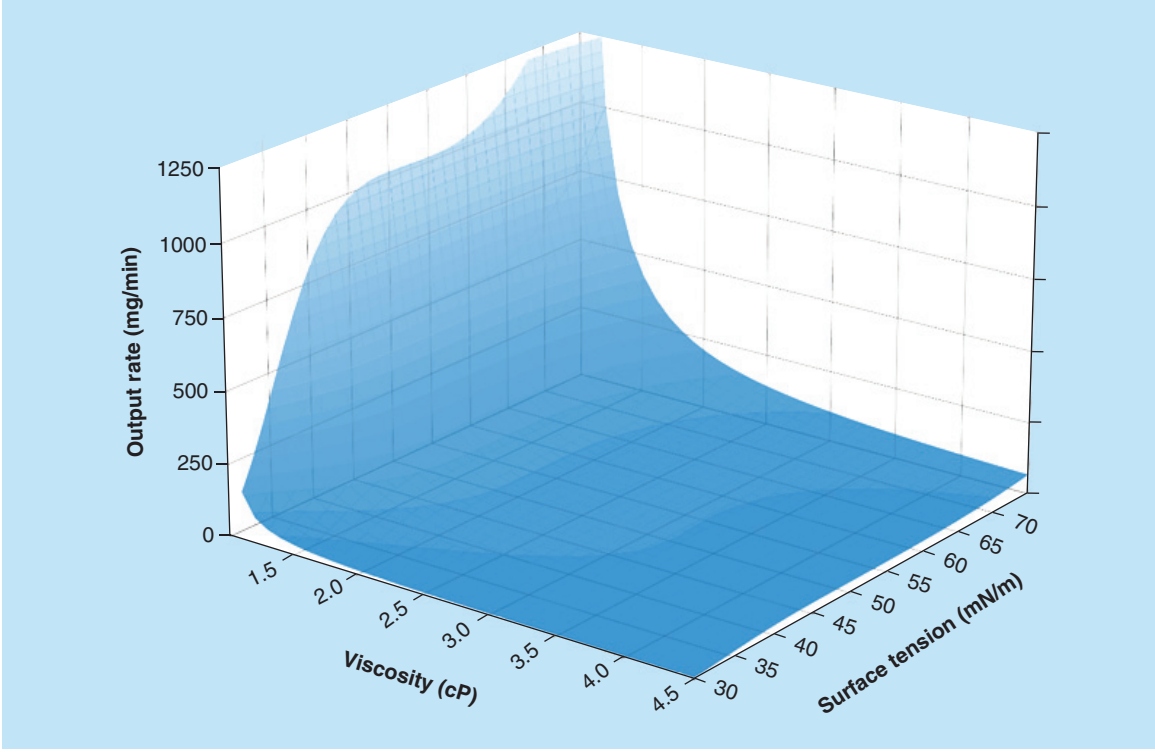

Figure 1. The influence of surface tension and viscosity on the output from a mesh nebulizer.
Reproduced with permission © RDD Asia 2016, Virginia Commonwealth University and RDD Online [55].

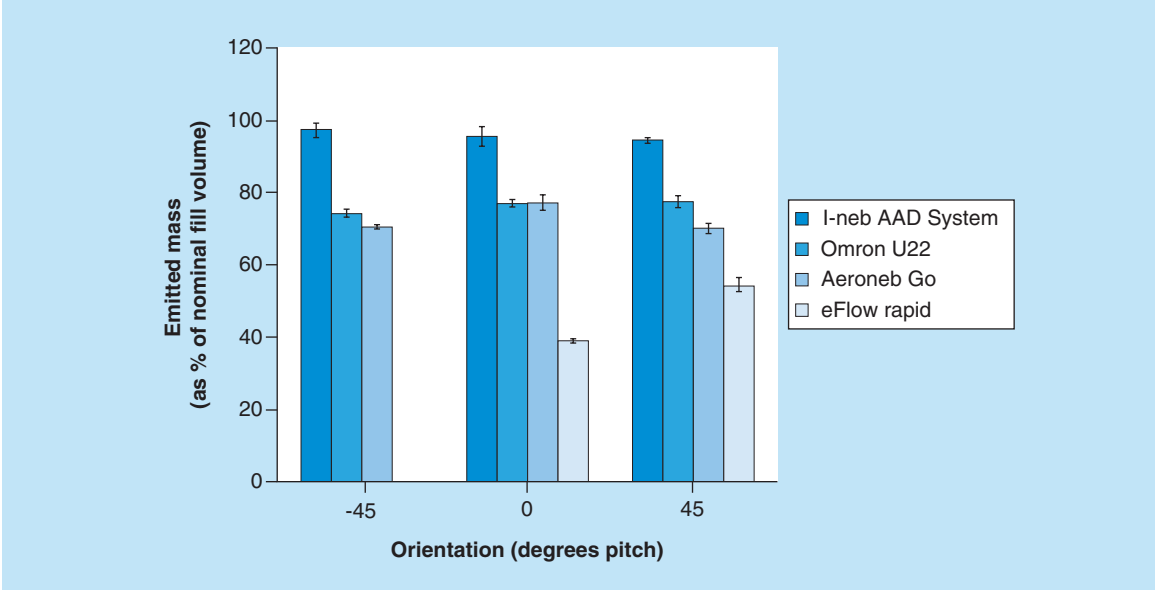

Figure 2. Effect of angle of operation upon the volume delivered from different mesh nebulizers.

patient, with fewer parts, easier cleaning and a more convenient design when in use. A recent example of such a device is the InnoSpire Go (Respironics Respiratory Drug Delivery [UK] Ltd) which has a simple two-piece construction that provides increased ease of drug loading, disassembly and cleaning (Figure 3). Early handling trials with a prototype device indicated that patients were able to clean and disassemble the device more easily than other leading mesh nebulizers [34].

In addition, manufacturing methods for the latest generation of mesh nebulizers will improve performance further; the mesh production process for the InnoSpire Go nebulizer incorporates in-process

controls to ensure that meshes produce consistent aerosol particle size and treatment times even after mesh replacement [35]. The selection of meshes to optimize droplet size for particular drugs or drug delivery requirements will also be possible [36].

Improving drug delivery

Drug delivery can be improved by using holding chambers or breath activation. Holding chambers store aerosol that would be wasted during the exhalation phase of breathing, ready for inhalation during the following breath. The size of the holding chamber and the characteristics of the breathing pattern will affect the improvement in drug delivery, but deposition of aerosol within the holding chamber means this is a less efficient means of improving drug delivery compared with breath activation. The electronics that form an inherent part of mesh nebulizer design allows the inclusion of sensors, feedback mechanisms and computational capability that can be used to provide features and functions, such as breath activation. A breath-activated nebulizer only generates aerosol during the inspiratory part of the breathing cycle. This minimizes the waste of aerosol during exhalation, and combined with the low residual volume of mesh nebulizers increases the efficiency of dose delivery. Efficient, repeatable dose delivery leads to the possibility and in some cases necessity of reducing the dose administered, which can reduce treatment time. Dose-delivery accuracy and minimization of treatment time are increased still further by the use of algorithms that predict the profile of the patient's next breath, based on earlier breaths, allowing compensation for device and anatomical dead space during aerosol delivery. Breath activation also reduces the need for an exhaled filter, which would otherwise be required to minimize the spread of antibiotics and other drugs into the local environment to prevent the accidental exposure of carers and others in the local vicinity during aerosol treatment. Audible, visual and tactile feedback have also been incorporated to allow the patient to interact with the device in order to facilitate drug delivery in the most efficient manner in terms of both high delivery to the lungs and the shortest possible timescale [37].

Adherence

Adherence to respiratory medication is low and is a key factor in lack of disease control [38]. Many factors influence this, including concerns about whether the drug and/or device are effective, so feedback from the device on correct operation can be important [38,39]. Poor technique also leads to poor outcomes, especially in a real-life setting. With a breath-activated mesh nebulizer, it is possible to log and time stamp when and how the device has been used, and upload the information to a server.

Figure 3. The InnoSpire Go mesh nebulizer.
Reproduced with the permission © Respironics Respiratory Drug Delivery (UK) Ltd.

An example of one such device, which allows for feedback to the patient to ensure correct technique and the recording of treatment data, is the I-neb Adaptive Aerosol Delivery (AAD) System device used with Insight Online (Respironics Respiratory Drug Delivery [UK] Ltd). A memory chip in the handpiece allows for the storing of treatment data, such as when the treatment took place, the length of treatment and the proportion of drug dose delivered. When connected to a computer with the Insight Online software and an internet connection, these data can be uploaded to a server accessible by the healthcare provider, and can therefore be used as a tool for remote healthcare and adherence monitoring [39,40]. Systems, such as I-neb Insight Online allow patients, physicians or support personnel, such as relatives to monitor, provide feedback or coach the patient to improve adherence and technique. Such an approach has been deployed in the care of cystic fibrosis patients in the UK, with the following benefits:

- Treatment times were reduced;
- Objective data were recorded;
- The number of doses taken correctly improved by approximately 20% [41];

10.4155/tde-2017-0015

- Improvements in adherence were sustained over 12 months;
- Lung function was better in patients with optimum adherence;
- Poor adherence resulted in increased use of healthcare resources;
- Motivational interviewing reduced the hospital use of intravenous antibiotics.

Future perspective

Recognizing the wide variability in delivered dose from different jet nebulizer/compressor combinations, regulatory authorities currently expect a new drug only to be promoted with nebulizers for which the developer has clinical experience. Increasingly, the drug market authorization will be via a specific drug–device combination product. The greater efficiency from breath-activated mesh nebulizers means that only 0.5 ml or less of the formulation needs to be nebulized, thereby significantly shortening treatment times.

Efficiency may be particularly important in the development of new drugs for nebulization, which may be costly to produce. This may be of particular relevance for the new generation of treatments involving macromolecules. Not only are such drugs expensive to manufacture, they are inherently less potent, thereby requiring doses beyond those that conventional inhalers are capable of delivering. Furthermore, fragments of DNA may require significant concentrations of excipient (up to ten-times the mass of drug) in order to achieve transfection of the target cell. Nebulizers are the only form of device capable of delivering such a payload for inhaled delivery [42], and high efficiency will be a major consideration in device choice. Furthermore, large doses will drive development of faster output nebulizers in order to maintain an acceptable treatment time. Due to their inherently efficient use of energy, mesh nebulizers are likely to lead the way. This might be through increased hole density, larger aperture plates or improved manufacturing processes [43–49].

Figure 4. The Micro soft mist device. Reproduced with the permission © Respironics Respiratory Drug Delivery (UK) Ltd.

There is also likely to be a significant drive to improve the current designs in order to improve key features, including ease of use, ease of cleaning, dose efficiency and connectivity. In particular, there is good evidence that encouraging a low inspiratory flow can improve lung deposition and peripheral penetration in diseased patients as well as reducing the treatment time for breath-actuated devices.

When lower doses are required, small volumes of liquid can be used to deliver the drug in only a few breaths, thereby creating the opportunity for a breath-activated soft mist device. The Micro (Respironics Respiratory Drug Delivery [UK] Ltd) is an example of such a device, which is currently in development for the delivery of inhaled insulin and other drugs (Figure 4). This innovative breath-actuated device precisely delivers a range of doses of up to 300 µl in fewer than eight breaths [50]. With less than 10% of the dose retained by the device and a high fine particle fraction [50,51], lung deposition can exceed 70% of the nominal dose [52]. It is reported that this can deliver as little as 50 µl with emitted dose in excess of 80% and a relative standard deviation of 2.8% [50], which would be delivered in one to two breaths. This performance is comparable to the Spiriva Respimat, which delivers one dose in two 22 µl puffs [53].

Mesh nebulizers are also being used in other new therapeutic areas, such as laparoscopic applications (AeroSurgical Limited, Galway, Ireland), to deliver medication to the peritoneal cavity [54]. Nevertheless, however good the device and drug are, the product will be ineffective unless the patient is motivated to take their medication.

Conclusion

In the future, state-of-the-art mesh nebulizers will become increasingly common and will increase the efficiency and consistency of nebulized aerosol delivery. Monitoring symptoms and capturing the data in the same system may offer even greater benefits, both by ensuring there is optimum treatment and by providing positive feedback to the patient to encourage proper adherence and management of their disease.

Acknowledgements

The author acknowledges N Smith (PS5 Consultants Ltd, Portsmouth, Hampshire, UK) for his editorial assistance.

Financial & competing interests disclosure

JN Pritchard is an employee of Philips Electronics UK Limited, who manufactures and sells nebulizers and valved holding chambers. He is also a minor shareholder in a number of pharmaceutical companies with interests in respiratory therapy. The author has no other relevant affiliations or financial involvement with any organization or entity with a financial interest in or financial conflict with the subject matter or materials discussed in the manuscript apart from those disclosed.

Executive summary

Nebulized therapy

- Nebulized therapy has universal applicability in the treatment of all respiratory patients due to the ability of patients to receive a dose of drug using their normal breathing cycle.
- It has been estimated that the use of nebulized therapy is growing faster than either pressurized metered dose inhaler or dry powder inhaler treatments.

Asthma & chronic obstructive pulmonary disease

- Asthma and chronic obstructive pulmonary disease (COPD) are the two most common respiratory diseases worldwide.
- Aerosol delivery via nebulization is of more significance in COPD due to the predominant elderly population.
- The prevalence of COPD is forecast to increase in the next few decades.
- The increase in COPD will drive the increased use of nebulized therapy even further due to the inability of the elderly to use inhalers.
- There is a dearth of long-acting β-agonist and long-acting muscarinic antagonist drugs in nebulized form, but there are signs this is now being addressed.
- There is potential for nebulized triple combinations of long-acting β-agonist, long-acting muscarinic antagonist and inhaled corticosteroids in the future.

Nebulizers in drug development

- Nebulizers have long been used in the early stages of drug development, but tended to be dropped for later stage development in favor of an inhaler.
- A new approach, where the nebulizer is taken through to market, with inhaler development in parallel during the later stages, may offer improved return on investment.

New nebulizer technology

- Mesh nebulizers are set to revolutionize nebulized therapy, with increased portability, quiet operation, rapid rates of aerosol delivery, low residual volumes and improved dose accuracy.
- Sales of mesh nebulizers are forecast to grow at three-times the rate of jet nebulizers in the next few years.
- The latest generation of mesh nebulizers will be easier to use, with fewer parts and easier cleaning.

Improving drug delivery

- Drug delivery can be improved by using holding chambers or breath activation.
- Breath activation in mesh nebulizers can increase dose delivery to the patient and minimize the waste of drug to the local environment.

Adherence

- Adherence to respiratory medication is low and is a key factor in lack of disease control.
- Poor technique also leads to poor outcomes.
- Remote healthcare and adherence monitoring can be used to improve adherence and technique.

The future of nebulized therapy

- Increasingly, the drug market authorization will be via specific drug–device combinations.
- Treatment times will become shorter as output rates are increased.
- Smart mist devices will allow delivery of some drugs within several breaths.
- State-of-the-art mesh nebulizers will provide feedback to the patient to improve their administration technique as well as providing adherence monitoring to allow the patient to optimize their treatment regimen.
- Future nebulizer designs may include symptom monitoring.

References

Papers of special note have been highlighted as:
•• of considerable interest

1 Nikander K, Saunders M. The early evolution of nebulizers. *Medicamundi* 54(3), 47–53 (2010).

2 United Nations Environmental Programme. June 2015 Report of the technology and economic assessment panel Volume 1. http://ozone.unep.org/en/teap-june-2015-progress-report-volume-1

3 Shen A. Market analysis of inhalation products for asthma and COPD in China. Presented at: *Management Forum*

Inhaled Drug Delivery. London, UK, 5–6 November 2014.

4 Vogelmeier C, Kardo P, Hofman T *et al*. Nebulised budesonide using a novel device in patients with oral steroid-dependent asthma. *Eur. Respir. J.* 45(5), 1273–1282 (2015).

5 Meiners S, Eickelberg O, Königshoff M. Hallmarks of the ageing lung. *Eur. Respir. J.* 45(3), 807–827 (2015).

6 World Heath Organisation. Life expectancy at birth (years), 2000–2015. http://gamapserver.who.int/gho/interactive_charts/mbd/life_expectancy/atlas.html

7 Saidi OE. Respiratory market stratification inevitable, augmented by ERS revelations. *Drug Deliv. Insight* 332(1), 3–5 (2014).

8 Mathers CD, Loncar D. Projections of global mortality and burden of disease from 2002 to 2030. *PLoS Med.* 3(11), e442 (2006).

9 You Y. The dynamics of the inhalation market in China. Presented at: *Inhalation Asia*. Shenyang, China, 9–11 September 2015.

10 Giraud V, Roche N. Misuse of corticosteroid metered-dose inhaler is associated with decreased asthma stability. *Eur. Respir. J.* 19(2), 246–251 (2002).

11 Sestini P, Cappiello V, Aliani M *et al.* Prescription bias and factors associated with improper use of inhalers. *J. Aerosol Med.* 19(2), 127–136 (2006).

12 Molimard M, Raherison C, Lamarque S *et al.* Real life assessment of inhaler use and acute exacerbations in 2935 COPD patients. *Eur. Respir. J.* 48(Suppl. 60), PA4078 (2016).

13 Taffet GE, Donohue JF, Altman PR. Considerations for managing chronic obstructive pulmonary disease in the elderly. *Clin. Interv. Aging* 9, 23–30 (2014).

14 Winningham RE. Theravance Biopharma. Presented at: *14th annual Needham Healthcare Conference*. New York, NY, USA, 14–15 April 2015. www.sec.gov/Archives/edgar/data/1583107/000110465915027343/a15--9036_1ex99d1.htm

15 Pritchard JN. Rethinking the paradigm for the development of inhaled drugs. *Int. J. Pharm.* 496(2), 1069–1072 (2015).

•• **A model showing the potential benefit of taking a nebulized formulation through to market in the drug development process.**

16 Pritchard JN. Accelerating the development of inhaled drugs. *Pharmaceutical Manufacturing and Packing Sourcer* (2005). http://solutions.3m.com/3MContentRetrievalAPI/BlobServlet?lmd=1219084613000&locale=en_WW&univid=1114280195952&fallback=true&assetType=MMM_Image&blobAttribute=ImageFile&placeId=19604&version=current

17 Pritchard JN. Maximizing the effectiveness of the inhaled drug development process. In: *Respiratory Drug Delivery 2016 (Volume 3)*. Dalby RN, Byron PR, Peart J *et al.* (Eds). Virginia Commonwealth University, VA, USA, 497–502 (2016).

18 Haumann BK, Nicholls AJ, Barnes C, Bourdet DL, Moran EJ. Dose-ranging study of once-daily TD-4208, an inhaled long-acting muscarinic antagonist (LAMA) in patients with chronic obstructive pulmonary disease (COPD). *Am. J. Respir. Crit. Care Med.* 191(meeting abstracts), A5750 (2015).

19 Franciosi LG, Diamant Z, Banner KH *et al.* Efficacy and safety of RPL554, a dual PDE3 and PDE4 inhibitor, in healthy volunteers and in patients with asthma or chronic obstructive pulmonary disease: findings from four clinical trials. *Lancet Respir. Med.* 1(9), 714–727 (2013).

20 Rau JL. Design principles of liquid nebulization devices currently in use. *Respir. Care* 47(11), 1257–1278 (2002).

21 Hess DR. Aerosol delivery devices in the treatment of asthma. *Respir. Care* 53(6), 699–725 (2008).

22 Pritchard JN. Back to the Future with Nebulized Therapy: New Opportunities in a Growing Market. In: *Respiratory Drug Delivery Asia 2016 (Volume 1)*. Dalby RN, Peart J, Young PM, Traini D (Eds). Virginia Commonwealth University, VA, USA, 15–24 (2016).

23 McCallion ONM, Patel MJ. Viscosity effects on nebulisation of aqueous solutions. *Int. J. Pharm.* 130, 245–249 (1996).

24 Rottier BL, van Erp CJ, Sluyter TS, Heijerman HG, Frijlink HW, Boer AH. Changes in performance of the Pari eFlow rapid and Pari LC plus during 6 months use by CF patients. *J. Aerosol. Med. Pulm. Drug Deliv.* 22(3), 263–269 (2009).

25 Perkins and Coates, Letters to the editor. Performance of PARI eFlow. *J. Aerosol. Med. Pulm. Drug Deliv.* 23(2), 113–114; author reply 114–118 (2010).

26 Bakuridze L, Andrieu V, Dupont C, Dubus JC. Does repeated disinfection of the e-Flow rapid nebulizer affect *in vitro* performance? *J. Cyst. Fibros.* 6(4), 309–310 (2007).

27 Gowda AA, Cuccia AD, Smaldone GC. Reliability of vibrating mesh technology. *Respir. Care* 62(1), 65–69 (2017).

28 Hardaker LE, Hatley RH. *In vitro* characterization of the I-neb Adaptive Aerosol Delivery (AAD) System. *J. Aerosol. Med. Pulm. Drug Deliv.* 23(Suppl. 1), S11–S20 (2010).

29 Ingram H. Nebulisers – World – 2014. https://technology.ihs.com/435839/nebulizers-2014

30 DiBlasi RM. Clinical controversies in aerosol therapy for infants and children. *Respir. Care* 60(6), 894–914 (2015).

31 Michotte JB, Jossen E, Roeseler J, Liistro G, Reychler G. *In vitro* comparison of five nebulizers during noninvasive ventilation: analysis of inhaled and lost doses. *J. Aerosol. Med. Pulm. Drug Deliv.* 27(6), 430–440(2014).

32 Michotte JB, Staderini E, Le Pennec D *et al. In vitro* comparison of a vibrating mesh nebulizer operating in inspiratory synchronized and continuous nebulization modes during noninvasive ventilation. *J. Aerosol. Med. Pulm. Drug Deliv.* 29(4), 328–336 (2016).

33 Goodman N, Morgan M, Nikander K, Hinch S, Coughlin S. Evaluation of patient-reported outcomes and quality of life with the I-neb AAD system in patients with chronic obstructive pulmonary disease. *J. Aerosol. Med. Pulm. Drug Deliv.* 23(Suppl. 1):S61–S70 (2010).

34 Hatley R, Rowe L, Rabbetts I, Quadrelli F. Optimizing patient experience of nebulizer treatments. *Eur. Respir. J.* 48(Suppl. 60), PA4082 (2016).

35 Hatley RHM, Hardaker LEA, Metcalf AP, Parker J, Quadrelli F, Pritchard JN. Ensuring the consistency of

performance of mesh nebulizers. Presented at: *Drug Delivery to the Lungs Conference 27*, Edinburgh, Scotland, UK, 7–9 December 2016.

36 Hatley R, Hardaker L, Zarins-Tutt J *et al.* Investigation of optical density for the characterization of nebulizer meshes. In: *Respiratory Drug Delivery 2016 (Volume 3)*. Dalby RN, Byron PR, Peart J *et al.* (Eds). Virginia Commonwealth University, VA, USA, 489–492 (2016).

37 Denyer J, Dyche T. The Adaptive Aerosol Delivery (AAD) technology: past, present, and future. *J. Aerosol Med.* 23(Suppl. 1), S1–S10 (2010).

38 Pritchard JN, Nikander K. Impact of intervention and feedback on adherence to treatment. In: *Respiratory Drug Delivery 2012 (Volume 1)*. Dalby RN, Byron PR, Peart J, Suman JD, Farr SJ, Young PM (Eds). Virginia Commonwealth University, VA, USA, 271–282 (2012).

39 Pritchard JN, Nicholls C. Emerging technologies for electronic monitoring of adherence, inhaler competence, and true adherence. *J. Aerosol Med. Pulm. Drug Deliv.* 28(2), 69–81 (2015).

•• **A paper highlighting the issues of adherence and inhaler competence, and discusses the technologies emerging for addressing these issues.**

40 Spencer T, Daniels T, Pollard K *et al.* I-neb Insight Online – a telemedicine option in the treatment of cystic fibrosis. *J. Cystic Fibros.* 11(Suppl. 1), S78 (2012).

41 Proceedings of I3: Innovation in Inhalation. Electronic Monitoring: the true value of true adherence. https://app.box.com/s/7hoohbfne2cmwtw6iv10l078hgwx02rs/1/8763078849/734569319291/1

42 Bohr A, Mortiz Beck-Brichsitter. Generation of tailored aerosols for inhalative drug delivery employing recent vibrating-mesh nebulizer systems. *Ther. Deliv.* 6(5), 621–636 (2015).

43 Hogan B. US0334338 A1 (2013).

44 Pumm G, Seifert R, Holzmann P, Brune N. US9168556 B2 (2015).

45 Schulz H, Holzmann P, Seidel D, Hahn M. US0263721 A1 (2014).

46 Hijlkema M, Pritchard JN, Sanders RHM, van der Schaft JC. WO2015011608 A1 (2015).

47 Lu CF, Chen CJ, Yang JC, Huang CH, Chiang HL. US7931356 B2 (2011).

48 Hsieh SP, Su YJ, Huang CC *et al.* US8870100 B2 (2014).

49 Yu NC, Zhen XZ, Xian T. EP1762264 A1 (2007).

50 Degtyareva Y, Metcalf A, Hardaker L, Pritchard JN, Hatley R. Efficiency of the Micro mesh nebulizer tested with three different fill volumes. In: *Respiratory Drug Delivery Europe 2015 (Volume 2)*. Dalby RN, Byron PR, Peart J, Suman JD, Young PM, Traini D (Eds). Virginia Commonwealth University, VA, USA, 401–404 (2015).

51 Parker J, Hardaker LEA, Hatley RHM. Performance of the Micro device with different inspiratory flow rates. Presented at: *Drug Delivery to the Lungs Conference 26*, Edinburgh, Scotland, UK, 9–11 December 2015.

52 Galindo VC, de Melo Barcelar J, Alcoforado L, Brandão SCS, Fink JB, de Andrade AD. Impact of breathing pattern on deposition and tolerability of a novel liquid inhaler. *J. Aerosol Med. Pulm. Drug Deliv.* 28(3), A26 (2015).

53 Spiriva Respimat (tiotropium bromide) inhalation spray. *Full prescribing information.* Ridgefield CT. Boehringer Ingelheim Pharmaceuticals, Inc.

54 Ingelmo PM, Bucciero M, Somaini M *et al.* Intraperitoneal nebulization of ropivacaine for pain control after laparoscopic cholecystectomy: a double-blind, randomized, placebo-controlled trial. *Br. J. Anaesth.* 110(5), 800–806 (2013).

55 Cullen S, Hibbitts A, Tajber L, MacLoughlin R, Cryan SA. Investigation of excipient properties on output rates in a vibrating mesh nebulizer. *J. Aerosol Med. Pulm. Drug Deliv.* 26(2), A-32 (2013).

Research Article

For reprint orders, please contact reprints@future-science.com

Future Medicinal Chemistry

Novel EGFR (T790M)-cMET dual inhibitors: putative therapeutic agents for non-small-cell lung cancer

Pankaj Kumar Singh[1] & Om Silakari*,[1]

[1]Molecular Modelling Lab (MML), Department of Pharmaceutical Sciences and Drug research, Punjabi University, Patiala, Punjab 147002, India

*Author for correspondence:
Tel.: +91 9501542696
Fax: +91 1752283075
omsilakari@gmail.com

Aim: Different resistance mechanisms, especially, T790M secondary acquired point mutation and in some cases amplification of cMET, have been a major setback for the lung cancer therapies. **Methodology:** The current *in silico* study explored the small molecules which can act as putative EGFR (T790M)-cMET dual inhibitors. Databases were first filtered and subsequently cross filtered, initially by thoroughly validated pharmacophore models for both targets. As per score and interactions obtained in docking, the molecules were subjected to molecular dynamics simulations, to study the stability and binding orientations of their complexes with target proteins. **Conclusion:** Molecular dynamics simulations predicted three hits to possess good binding affinities and stability for EGFR (T790M) and cMET, which can be claimed to be potential dual inhibitors.

First draft submitted: 16 December 2016; Accepted for publication: 2 February 2017; Published online: 31 March 2017

Keywords: cMET • EGFR (T790M) • lung cancer • molecular dynamics • pharmacophore

Even though rigorous research has been done for years, lung cancer still exists as one of the prevalent forms of cancer, with around 1.35 million patients per year. It also remains the reason for high rate of cancer-related mortality worldwide [1]. Out of the two, non-small-cell lung cancer (NSCLC) is more commonly observed subtype of lung cancer, which forms almost 85% of the total lung cancer cases [2]. Mutations leading to activation of the EGFR are observed in almost 30–40% of NSCLC patients. Patients with L858R mutation in EGFR, usually show positive response upon administration with first-generation reversible tyrosine kinase inhibitors (TKIs) [3].

However, after 9–14 months, disease advancement reoccurs, the impressive positive effects of erlotinib or gefitinib therapy fades, majorly due to an acquired mutation or secondary mutation in EGFR that leads to replacement of the gatekeeper residue threonine with methionine at 790 (T790M) in approximately 60% of cases [4]. Initially steric hindrance was considered to be the mechanism of how T790M secondary mutation causes resistance toward first-generation TKI's but recent studies disclosed that T790M secondary mutation enhances EGFR binding affinity for ATP, thus, leading to the competitive 'inhibition' of the inhibitors and reinstating its enzymatic function and rendering the first-generation inhibitors inactive [5]. Approaches targeting EGFR T790M mutation led to the development of second-generation inhibitors like dacomitinib, etc., which inhibit EGFR covalently but clinical studies revealed their nonselectivity toward the wild-type EGFR. Thus, significant toxicities are observed with these second-generation inhibitors, implying the need to develop or identify inhibitors with potential activity against T790M EGFR, without the toxicity of covalent inhibitors [6].

Also, there is another cross-talk mechanism which renders first-generation inhibitors inactive against NSCLC, that is, amplification of cMET. Similar to solid tumors, around 70%

FUTURE SCIENCE part of fsg

of NSCLC cases also show overexpression of cMET [7]. cMET activation leads to various cellular and subcellular functions such as proliferation, increased survival, etc [8]. Studies have shown role of cMET amplification in ERBB3-dependent activation of PI3K, leading to gefitinib resistance [9]. In majority of the cases, cMET amplification is not observed prior to the treatment with first-generation EGFR inhibitors. Clinical studies have shown that *in vitro* resistance developed due to cMET amplification to erlotinib and gefitinib lies in the range of 5–10 μM. Interestingly studies revealed that in about half of the patients having cMET amplification, acquired resistance due to T790M secondary mutation is observed either in same or different biopsy of the patient [10]. Further studies disclosed that blockade of cMET signaling by RNA interference led to revival of sensitivity of NSCLC toward gefitinib, and other molecules targeting EGFR and cMET, leading to efficient overpowering of resistance in the cMET-amplified EGFR TKI-resistant tumors. In addition, experimental and biochemical studies also revealed direct interaction between EGFR and cMET making them simultaneously targetable (Figure 1) [11].

Thus, current knowledge regarding NSCLC reveals the fact that it is imperative to design molecule/s which can inhibit EGFR with T790M secondary mutation, along with other signaling proteins such as cMET, which are involved in cross-talk mechanisms. Hence, in the current study, the commercial Asinex, Chembridge and Maybridge databases were screened using pharmacophore models, developed from EGFR (T790M) and cMET inhibitors which were obtained from the literature. The hits were then screened on the basis of their fitness values and further exposed to docking to remove poor hits from total retrieved hits. Further, the screened candidates were clustered on the basis of structural similarity. Finally, the molecules were studied via molecular dynamics simulations to validate the steadiness and interactions between lead molecules and the proteins. Here, authors have explored, using *in silico* tools, small heterocyclics possessing affinity toward resistant EGFR and cMET targets, for their possible role in NSCLC.

Materials & methods

Dataset

In this study, a total of 109 EGFR (T790M) and 90 cMET inhibitors were obtained from the literature comprising diverse series of compounds [12–29]. Focus was laid on the fact that all the compounds followed the same mechanism of action and employed similar experimental procedures for calculating biological activity. For the building up of pharmacophore models, activity of the compounds under consideration was expressed as IC_{50} values (μM). Out of these molecules, 16 compounds for EGFR (T790M) and 19 compounds for cMET were randomly chosen as training set compounds and rest of the molecules from each set were kept as the test set. The selected molecules were then prepared using the Prepare Ligands module in Discovery Studio (DS), and in which the molecular geometry is calculated with the CHARMm forcefield, and energy threshold is kept 20 kcal/mol, and default values are used for other parameters.

HypoGen-based pharmacophore models were built employing DS 4.1 [30]. CDOCKER was used to execute molecular docking studies [31], and finally, molecular dynamics simulations were run on computer terminal using Desmond software, version 3.8, due to unavailability of molecular dynamics feature in our DS package [32]. Molecular modeling studies were initiated with the selection of two proteins: EGFR (T790M) and cMET. In case of EGFR, human-derived structures of EGFR with T790M secondary acquired mutation were retrieved from the Protein Data Bank (PDB). Resolution value 2.50 Å was used as a filter, six protein structures were selected (Supplementary Table 1). Out of them, on the basis of cross docking, a process to determine the docking sensitivity by putting all ligands into all receptors of the target protein (Supplementary Table 8), PDB ID: 3W2P, 2.05 Å was found to have the lowest average Root mean square deviation (RMSD) and thus, selected for further analysis. Likewise, for cMET, more than 25 PDB structures were retrieved, out of which, 11 protein structures having resolution less than 2.00 Å were selected (Supplementary Table 2). Again, based on cross docking (Supplementary Table 9), PDB ID: 3DKF, 1.8 Å was found to have the lowest average RMSD and also, it possessed activating mutations responsible for amplification of cMET in lung cancer, thus, selected for analysis. In the next step, selected proteins were prepared using the protein preparation module in DS. This protocol uses the CHARMm forcefield to perform functions, such as, insertion of missing atoms, handling missing loops, removal of water and for filling the gap present in the protein structure.

Pharmacophore modeling & validation

HypoGen-based 3D-QSAR pharmacophore models were developed employing DS. In pharmacophore generation process, for the EGFR (T790M) and cMET inhibitors, the uncertainty value was kept three, representing the degree of uncertainty in the activity values and activity attribute of the molecules was characterized as active, moderately active and inactive. The pharmacophore mapping features such as hydrogen-bond acceptor (HBA), hydrophobic (HY), hydrogen-bond donor (HBD), ring aromatic (RA) and positive/negative ionizable were assigned values between a range of

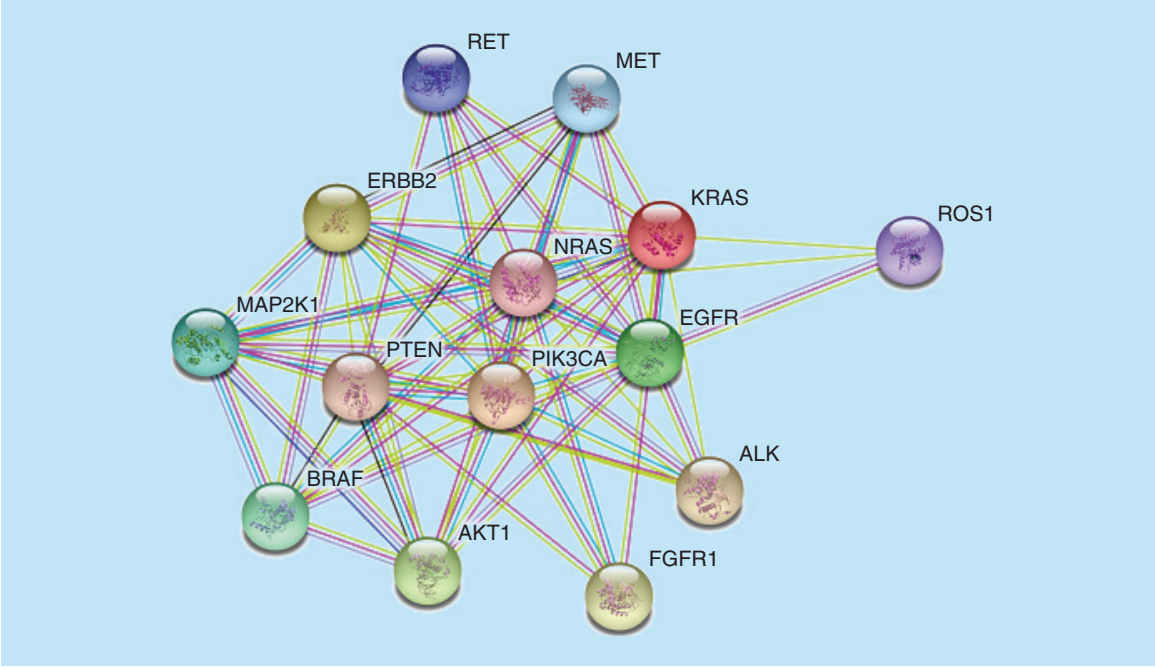

Figure 1. Protein–protein interaction diagram of EGFR–cMET interaction extracted from string database.

0–5, keeping the minimum inter-feature distance of 3.5 Å, for constructing the quantitative 3D pharmacophore model [33]. This methodology resulted in the development of a total of ten quantitative pharmacophoric hypotheses, which were judged based on the criteria such as cost values, correlation (R^2) and RMSD values. Cost analysis includes values such as fixed cost, which signify the least intricate model that fits in the data perfectly and total cost which is the total sum value of the error cost, weight cost and configuration cost. The null cost assumes that no relationship exists in between the calculated and observed bioactivities.

Out of the ten generated models, the most optimum model was picked up considering various parameters such as R^2 value, test set prediction and cost difference. The selected pharmacophore models were further validated by successive validation methods such as enrichment factor (EF) and goodness of hits (GH) score, Fischer's randomization test and receiver operating characteristic (ROC) curve. The Fischer's method calculates the actual correlation between structural attributes of the molecule and the reported biological activity and thus, attempts to nullify the prospect of chance correlation. In Fischer randomization, we challenge the computer to generate the superior hypothesis by feeding wrong data, to judge if there is any chance of R^2 and to assess whether exact R^2 occur between structure and activity. Further, external prediction was calculated using test set molecules by categorizing them according to their own variety of activity. This prediction was performed using flexible fitting option, which allows superimposition of the molecules over predefined pharmacophore features, considering the torsional degrees of freedom, available in the pharmacophore mapping module of DS. The selected models were then validated by calculating EF and GH score. The EF value defines the tendency of the models to preferentially pick the active over the inactive, while the calculation of GH value involves filtering a known database of active and inactive molecules by selected models.

$$EF = \left(\frac{Ha}{Ht}\right) \Big/ \left(\frac{A}{D}\right) \quad (1)$$

$$GH = \left\{\frac{[Ha * (3A + Ht)]}{4HtA}\right\} * \left[1 - \frac{Ht - Ha}{D - A}\right] \quad (2)$$

Furthermore, the selected models were validated using the calculation of sensitivity, specificity and ROC. ROC analysis assesses ability of the pharmacophore model to correctly classify a list of compounds as either active or inactive. The best pharmacophore model is considered to be the one which is able to segregate active molecules from inactive molecules. ROC of pharmacophore is showed by the AUC of the corresponding curve [34].

Virtual screening protocol

The pharmacophore-based virtual screening is ligand-based screening which involves screening of large databases of molecules having specific features essential for the selected target. Pharmacophore screening was performed to detect common features which are present in active molecules and are responsible for their activity, while, docking analysis was

Table 1. Cost analysis and correlation data for the pharmacophore hypothesis of EGFR (T790M).

Hypothesis	Total cost	Error cost	RMS	Correlation	Feature
$EGFR1_{ADHH}$	71.89	56.29	0.55	0.96	HBA, HBD, HY, HY
$EGFR2_{ADHH}$	73.90	58.31	0.73	0.93	HBA, HBD, HY, HY
$EGFR3_{AAHH}$	74.20	58.72	0.78	0.92	HBA, HBA, HBD, HY
$EGFR4_{ADDH}$	74.28	58.97	0.79	0.92	HBA, HBD, HBD, HY
$EGFR5_{ADDH}$	74.81	58.98	0.81	0.92	HBA, HBD, HBD, HY
$EGFR6_{ADHH}$	75.03	59.58	0.84	0.91	HBA, HBD, HY, HY
$EGFR7_{ADDH}$	75.67	60.19	0.89	0.90	HBA, HBD, HBD, HY
$EGFR8_{AADH}$	75.78	60.22	0.90	0.90	HBA, HBA, HBD, HY
$EGFR9_{AADH}$	75.81	60.27	0.90	0.90	HBA, HBA, HBD, HY
$EGFR10_{ADHH}$	76.06	60.53	0.91	0.90	HBA, HBD, HY, HY

Null cost = 89.43, fixed cost = 69.21, configuration cost = 14.27, all costs are in units of bits.
All pharmacophores consist of four features including HBA, HBD, HY and RA.
HBA: Hydrogen-bond acceptor, HBD: Hydrogen-bond donor, HY: Hydrophobic; RA: Aromatic ring; RMS: Root mean square deviation.

performed as a tool for structure-based screening, to point out the candidates who possess the conserved interaction with both EGFR (T790M) and cMET protein. Databases, namely Asinex (296,321), Chembridge (49,962) and Maybridge (54,262), were first screened by EGFR (T790M) and cMET pharmacophore models and then retrieved results were cross screened by both the models. This step led to the retrieval of molecules possessing the features of both the selected pharmacophore models. The 'Maximum Omitted Features' option was kept at one for the filtering of the databases so that only those compounds are obtained which consist of almost all the pharmacophoric assets. Compounds with good fitness score were forwarded for molecular docking analysis using CDOCKER.

Docking & molecular dynamics simulation

CDOCKER module in DS 4.1 was utilized to study the molecular interactions [31], which is based on the CHARMm-based forcefield. In CDOCKER, random conformations of ligands are generated and then, optimized in the binding site using rigid body rotations followed by simulated annealing. The main reason for using CDOCKER was the parallel job feature available with it. Thousands of molecules were to be docked at a time and CDOCKER provides advantage over other tools as it can perform parallel jobs. Protein crystal structure of EGFR (T790M) protein (PDB: 3W2P) and cMET protein (PDB: 3DKF), respectively, were extracted from protein data bank. The obtained poses were analyzed for any absence/presence of hydrogen bonding, RA, HY and

Table 2. Cost analysis and correlation data for the pharmacophore hypothesis of cMET.

Hypothesis	Total cost	Error cost	RMS	Correlation	Feature
$cMET1_{DHHR}$	87.15	68.89	0.72	0.95	HBD, HY, HY, RA
$cMET2_{DHHR}$	87.50	67.92	0.65	0.96	HBD, HY, HY, RA
$cMET3_{DHHR}$	87.71	67.74	0.63	0.96	HBD, HY, HY, RA
$cMET4_{DHHR}$	87.85	69.54	0.77	0.94	HBD, HY, HY, RA
$cMET5_{DHHR}$	87.86	67.93	0.73	0.95	HBD, HY, HY, RA
$cMET6_{DHHR}$	88.59	68.06	0.67	0.96	HBD, HY, HY, RA
$cMET7_{DHRR}$	88.96	70.70	0.84	0.93	HBD, HY, RA, RA
$cMET8_{DHHH}$	89.61	70.23	0.88	0.92	HBD, HY, HY, HY
$cMET9_{DHHR}$	89.63	70.49	0.83	0.93	HBD, HY, HY, RA
$cMET10_{ADHH}$	89.87	71.57	0.90	0.92	HBA, HBD, HY, HY

Null cost = 118.52, fixed cost = 82.17, configuration cost = 17.13, all costs are in units of bits.
All pharmacophores consist of four features including HBA, HBD, HY and RA.
HBA: Hydrogen-bond acceptor, HBD: Hydrogen-bond donor, HY: Hydrophobic; RA: Aromatic ring; RMS: Root mean square deviation.

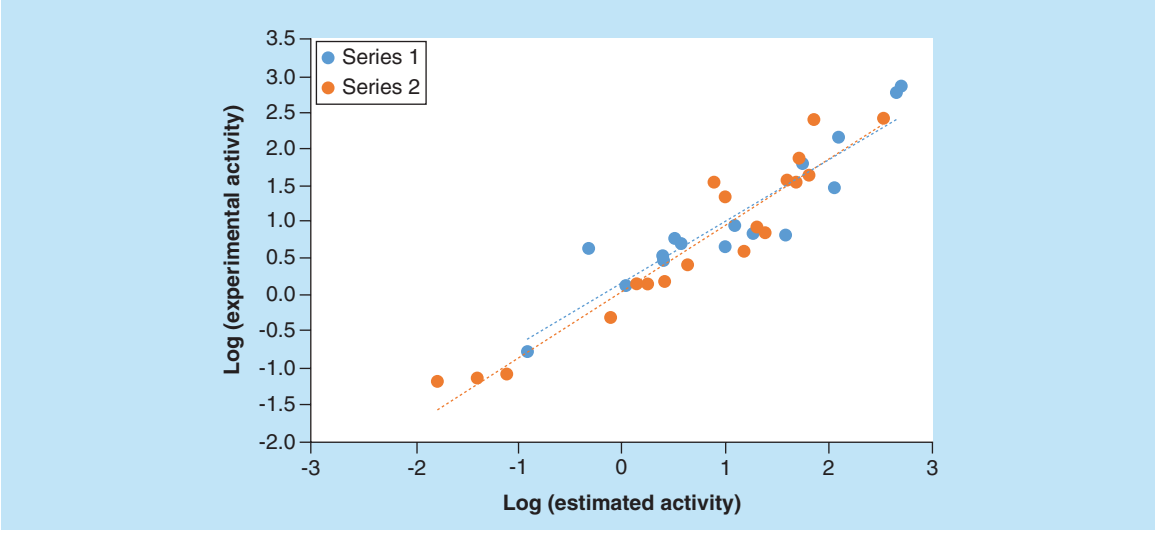

Figure 2. Correlation between experimental and estimated activities of training set compounds of $EGFR4_{ADDH}$ (Series 1) and $cMET1_{DHHR}$ (Series 2).

π–π interactions between the obtained hits and the protein cavity. After selection of molecules with good interaction with respective proteins, the docked molecules with respective EGFR (T790M) and cMET proteins were forwarded for the molecular dynamics simulations using OPLS_2005 forcefield based Desmond software, because of its better graphical user interface [35]. The simulations were performed to stabilize the protein–molecule complex and study the most stable interactions which are retained after the simulation time period of 10 ns, by observing its simulation-interaction diagram. Protocol of molecular dynamic simulations involved system building using TIP3P as solvent model and an orthorhombic box shape, the pH was adjusted by adding Na^+ ions and keeping salt concentration at 0.15 M. Then the simulation job was run keeping the temperature at 310 K, pressure of 1.01325 bars, and a time step of 1.0 fs, for a total of 10 ns.

Results & discussion

Pharmacophore model generation

A total dataset containing 109 EGFR (T790M) and 90 cMET inhibitors with experimental IC_{50} values, which were divided as training and test set was selected. Training set constituted of 16 EGFR (T790M) and 19 cMET inhibitors and rest of the inhibitors were kept as test set (Table 1).

Training set molecules were then exhausted to carry out pharmacophore analysis, conformer generation was performed using BEST method. After analysis, ten best hypotheses were generated and ranked according to their 'total cost'. All the hypothesis consisted of four features, rather than five features. The reason for this could be the number of features extracted from the best molecules present in the active molecules of the training set. Other reason can be removal of fifth feature during the subtraction step of the pharmacophore generation due to the presence of that feature in the inactive molecules of the training set. Also, literature suggested that any statistically validated four feature pharmacophore is as significant as a validated five feature pharmacophore. The most optimum pharmacophore hypothesis for EGFR, $EGFR4_{ADDH,}$ which consists of four features: HBA, two HBD and HY, was chosen. Theoretically, it is expected to pick the best hypothesis on the basis of cost analysis only and thus, researchers usually pick out the first hypothesis out of the generated ten hypotheses, in this case EGFR1. However, as in DS, test set validation occurs in same step as model generation, thus, in our work we took R^2 and test set prediction values along with cost analysis to pick the best hypothesis. Both EGFR1 and $EGFR4_{ADDH}$ were having comparable cost analysis values and R^2 but EGFR1 had test set prediction value (0.59) lower than $EGFR4_{ADDH}$ test set prediction value (0.72). For cMET, $cMET1_{DHHR}$ consisted of four features: HBD, two HY and RA. All the generated hypotheses for EGFR (T790M) and cMET with their parameters, are given in Tables 2 & 3, respectively.

The hypothesis $EGFR4_{ADDH}$ showed the nullcost and total cost value to be 89.43 and 74.28 bits and null cost to fixed-cost difference to be 20.22, with the R^2 coefficient value of 0.92. This indicates that the hypothesis $EGFR4_{ADDH}$ is best suited for predictability. Similarly the hypothesis $cMET1_{DHHR}$ showed null cost and total cost value to be 118.52 and 87.15 bits, and null cost to fixed-cost difference to be 36.35

bits, with the correlation coefficient (R^2) value of 0.95 (Figure 2).

Both the selected pharmacophoric hypotheses mapped completely onto the respective most active molecule of the dataset and these showed the fit values of 8.13 and 8.10 for $EGFR4_{ADDH}$ and $cMET1_{DHHR}$, respectively. The hypothesis selected for EGFR (T790M) contains two HBD, one HBA and one HY group (Figure 3A). Upon mapping over the most active molecule, hypothesis (EGFR, Supplementary Table 3) showed that the two donors and one acceptor features overlap the two NH substitutions and one N of the pyrimidine ring of the molecule (Figure 3B). The hypothesis selected for cMET consists of two HY, one HBD and one aromatic ring (Figure 3C). Upon mapping over the most active molecule, it showed that the donor feature overlaps the NH substitution of the molecule (cMET, Supplementary Table 4); the HY feature occupies the pyrazine ring; the aromatic ring feature overlaps the fused pyridine ring (Figure 3D). The mapping of the training set and test set molecules provided the estimated activities against $EGFR4_{ADDH}$ and $cMET1_{DHHR}$, shown in Supplementary Tables 3, 4, 5 & 6.

Pharmacophore model validation

The pharmacophore models were thoroughly validated to identify the finest model that can recognize the active hits during screening. Fischer randomization at CI 99% was performed and 99 spreadsheets were generated. None of the spreadsheet showed cost value better than the best one ($EGFR4_{ADDH}$ and $cMET1_{DHHR}$). The external test set prediction was performed for both targets, the result displayed R^2_{pred} value of 0.724 and 0.692 for $EGFR4_{ADDH}$ and $cMET1_{DHHR}$, respectively. Further validation was carried out by calculating the EF and GH value for the database of 290 and 396 known EGFR (T790M) and cMET inhibitors, containing 96 and 100 active, and 194 and 296 inactive molecules. The $EGFR4_{ADDH}$ and $cMET1_{DHHR}$ gave an EF score of 2.33 and 2.62, respectively (Supplementary Table 7) and GH score was found to be 0.696 and 0.593 for EGFR (T790M) and cMET, respectively. Further ROC parameter of both the models, $EGFR4_{ADDH}$ and $cMET1_{DHHR,}$ was determined by calculating the selectivity and specificity. Sensitivity represents the ability of a model to detect true positives while, specificity represents

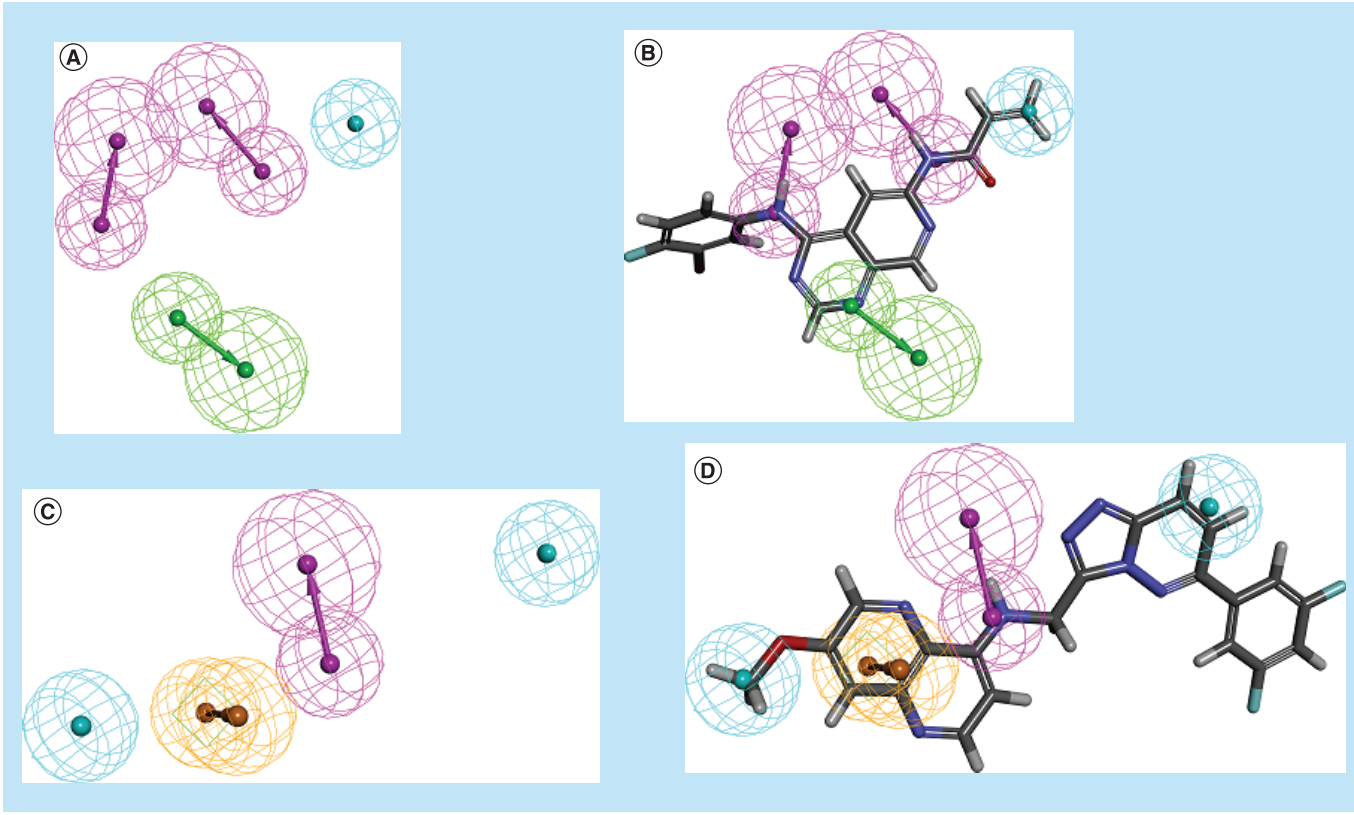

Figure 3. Analysis of generated pharmacophore hypothesis for both targets. The best pharmacophore model **(A)** Hypo4 of EGFR (T790M) contains two hydrogen bond donors (magenta), one hydrogen bond acceptor (green) and one hydrophobic (HY: blue). **(B)** Hypo1 of cMET contains one hydrogen bond donor (magenta), one aromatic ring (orange) and two hydrophobic (blue). **(C)** Alignment of Hypo4 of EGFR (T790M) over the most active compound. **(D)** Alignment of Hypo1 of cMET over the most active compound.

Table 3. 2D structures of hits screened with estimated activities of EGFR (T790M) and cMET.

Code	Structure	Estimated activity EGFR (T790M)	Estimated activity cMET	MM-GBSA (EGFR [T790M])	MM-GBSA (cMET)
ASN 06744373	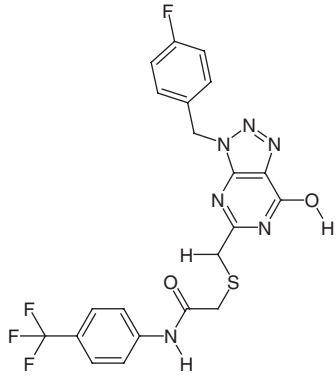	0.006	0.004	-53.13	-76.51
BAS 00366743	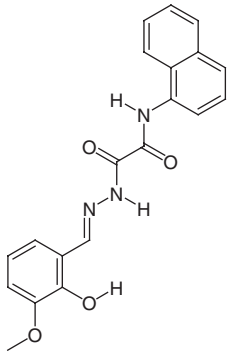	0.064	0.004	-35.22	-70.89
ASN 04450511	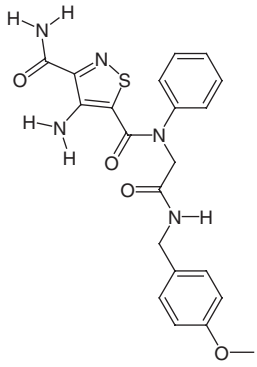	0.080	0.008	-53.98	-71.10
BAS 09867482	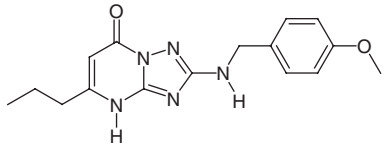	0.029	0.010	-63.11	-61.38

Table 3. 2D structures of hits screened with estimated activities of EGFR (T790M) and cMET (cont.).

Code	Structure	Estimated activity EGFR (T790M)	Estimated activity cMET	MM-GBSA (EGFR [T790M])	MM-GBSA (cMET)
BAS 01516645	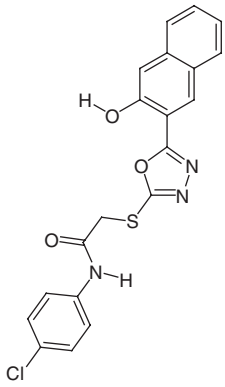	0.026	0.012	-64.43	-76.56
BAS 02496009	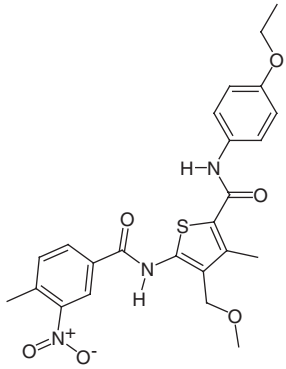	0.013	0.020	-70.82	-83.87
ASN 11105444	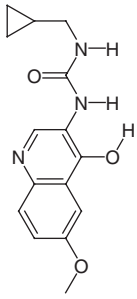	0.036	0.029	-50.49	-79.17
MCFD02678814	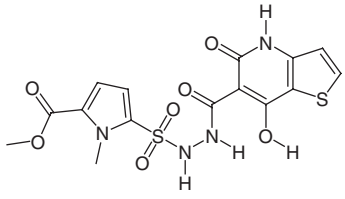	0.059	0.027	-52.17	-67.61

Table 3. 2D structures of hits screened with estimated activities of EGFR (T790M) and cMET (cont.).

Code	Structure	Estimated activity EGFR (T790M)	Estimated activity cMET	MM-GBSA (EGFR [T790M])	MM-GBSA (cMET)
BAS 00600420	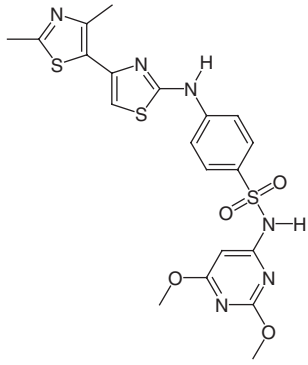	0.079	0.008	-61.32	-80.16
ASN 05338515	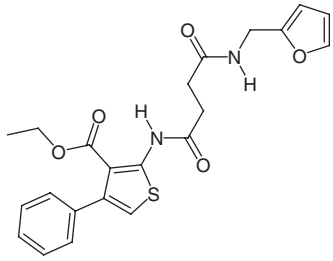	0.026	0.006	-71.76	-69.29
BAS 12240138	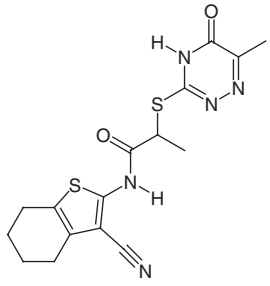	0.037	0.019	-66.50	-70.67

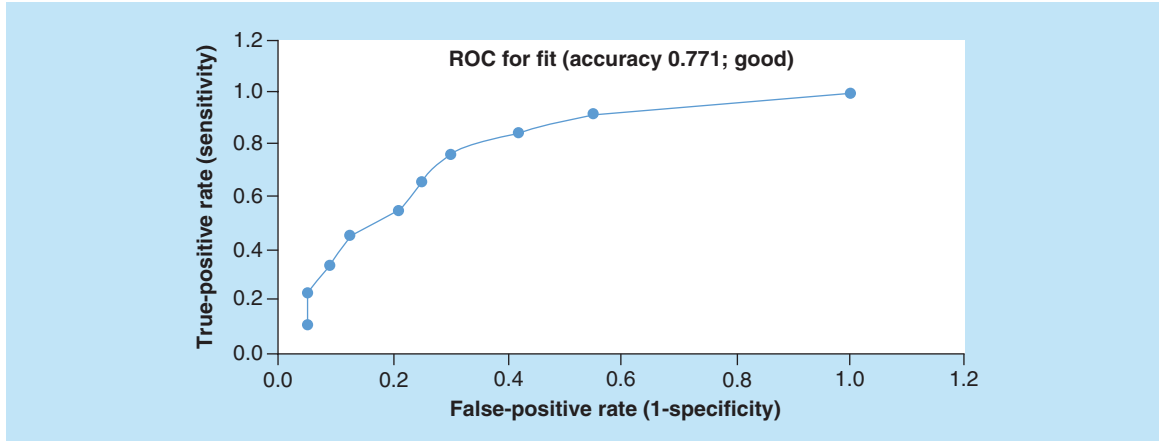

Figure 4. Receiver operating curve generated during validation of $EGFR4_{ADDH}$.
ROC: Receiver operating curve.

the ability to prevent false positives. Determination of ROC score requires calculation of AUC. ROC analysis of $EGFR4_{ADDH}$ resulted in the score of 0.771 (Figure 4), and of $cMET1_{DHHR}$ resulted in the score of 0.818, which were significantly above the cut-off value of 0.5 (Figure 5). These validation procedures provided enough evidence on both $EGFR4_{ADDH}$ and $cMET1_{DHHR}$, respectively.

Further a sequential virtual screening procedure was employed. Pharmacophoric features in the models provided the first line of screening for the commercially available small molecule databases. The databases were then, on second step, screened out depending upon the fit value obtained via pharmacophore mapping. Molecules with fitness score above 6.0 in EGFR (T790M) and 6.6 in cMET, were selected. These obtained molecules were then cross-screened, that is, molecules from the $EGFR4_{ADDH}$ were filtered through $cMET1_{DHHR}$ and vice versa to obtain dual applicability molecules.

Molecular docking analyses & molecular dynamic simulations

Docking of hits from cross-screening against both EGFR (T790M) and cMET was performed. In this step, first the PDB selection was done considering the results of cross docking and resolution of PDB, which led to selection of 3W2P and 3DKF from PDB database, for EGFR (T790M) and cMET, respectively. After visual examination, 275 compounds showing key interactions were selected based on the active site requirements and information gained from existing inhibitors. On analysis of these molecules, it was observed that in docking they were able to maintain binding interactions essential for EGFR (T790M) and cMET active site and also, followed orientations

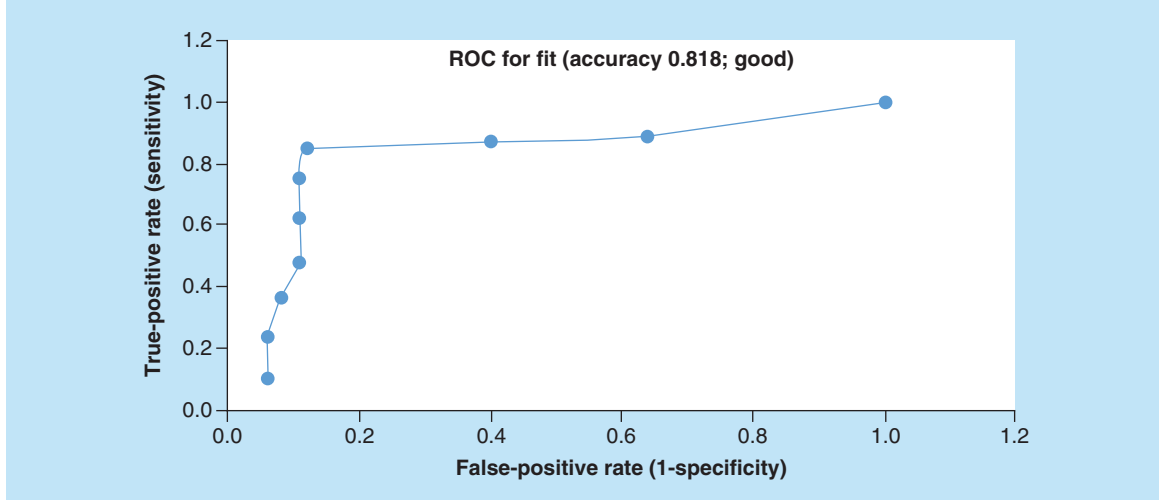

Figure 5. Receiver operating curve generated during validation of $cMET1_{DHHR}$.
ROC: Receiver operating curve.

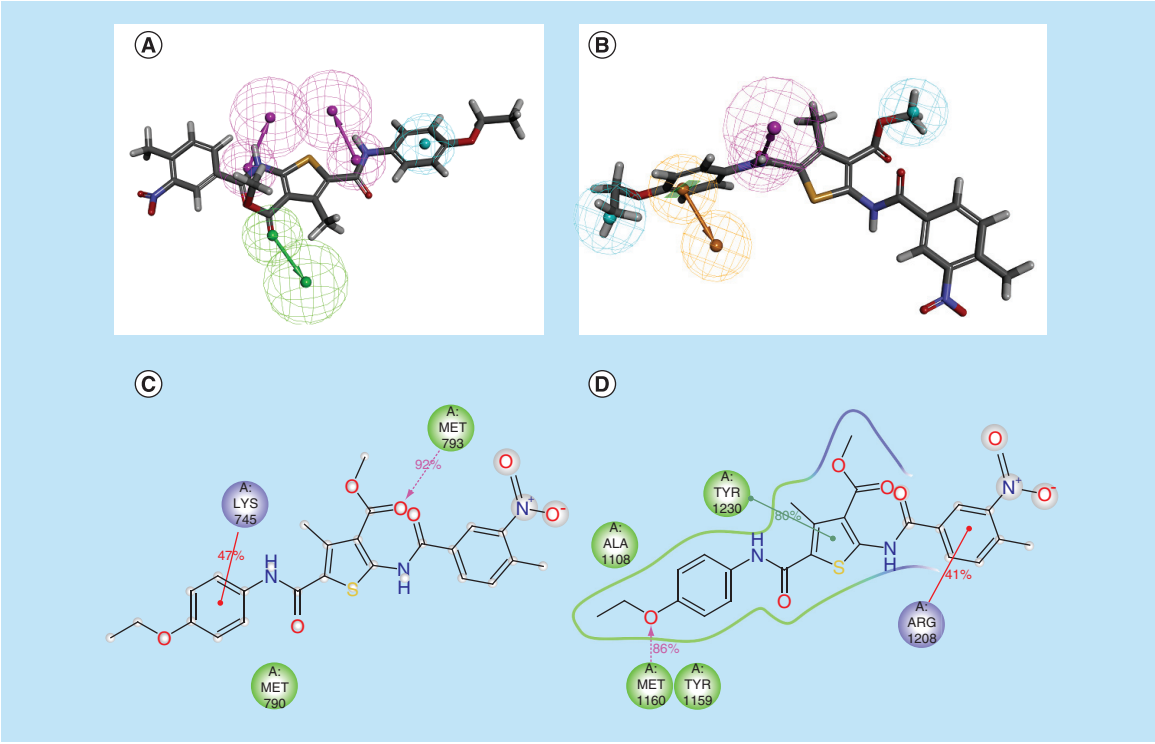

Figure 6. Pharmacophore and molecular dynamics analysis result of top-most molecule. Final best-hit compound mapped onto the best pharmacophore models of **(A)** EGFR (T790M), **(B)** cMET. The hydrogen-bond acceptor, hydrogen-bond donor, aromatic ring and hydrophobic features are displayed in green, magenta, orange and cyan, respectively. Molecular dynamics simulation results of the best-hit compound with proteins of **(C)** EGFR (T790M) and **(D)** cMET.

present in the selected pharmacophore models. Out of the retrieved molecules, the best hit mapped with the EGFR (T790M) and cMET pharmacophore models are shown in Figure 6A & B. To reduce the number of molecules for further analysis, similar structurally attributed molecules were removed by clustering on the basis of structural features, which yielded 11 molecules (Table 4).

In the last step, molecular dynamics simulations were run to analyze and validate the interactions, stability and binding of the retrieved hits with their proteins. Thus, retrieved molecule formed putative 11 dual inhibitors, 22 complexes, with both EGFR (T790M) and cMET proteins. These complexes were exposed to molecular dynamics (MD) simulations for a time frame of 10 ns. Careful investigation of simulation-interaction diagrams revealed overall three molecules to retain the conserved interactions in both the proteins, which are essential for inhibitory activity, thus, justify the claim of dual inhibitors. Furthermore, to validate the obtained results, protein–ligand complexes were analyzed for their stability by calculating the RMSD between protein backbones and the best molecule, as shown in Supplementary Figure 1A & B. The values were found in the range of 0.5–3.5 Å for proteins and 0.8–4.0 Å for the ligands. Few variations in RMSD can be justified by the fact that slight adjustment occurs in the beginning of a simulation study. However, RMSD and interactions within the active site of both the protein molecules conclude that complex was fairly stable after initial adjustment. The best retrieved molecule possessed conserved hydrogen bond interactions with ATP domain amino acid Met793 (92% of the interaction was maintained after the time interval of 10 ns) of EGFR (T790M) protein (Figure 6C), which is crucial for a molecule to be considered as an EGFR inhibitor. It also possessed HY interaction with Lys745, which was stable throughout time frame of 10 ns. Same hit also showed hydrogen bonding with Met1160 (86% of the interaction was maintained after the time interval of 10 ns), 80% of the π–π interaction was maintained with Tyr1230 providing stability to the ligand in the kinase domain and 41% of the HY interaction with Arg1208 was maintained at the kinase domain of cMET (Figure 6D).

Finally, MM-GBSA method was employed to determine the relative affinity of the best hits with EGFR (T790M) and cMET proteins (Table 4). Results showed the binding energy value of -90.69 kcal/mol for EGFR (T790) best-hit complex and -72.26 kcal/mol for cMET best-hit complex. At last the final hits were subjected for the evaluation of toxicity, using toxicity prediction module of DS. This module predicts the Ames mutagenicity

Table 4. Toxicity prediction data of the final hits for EGFR (T790M) and cMET.

Code	Structure	TOPKAT Ames prediction	TOPKAT Ames score
ASN 05338515	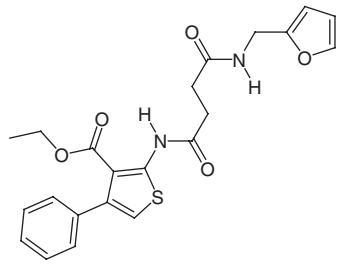	Nonmutagen	-8.44
BAS 02496009	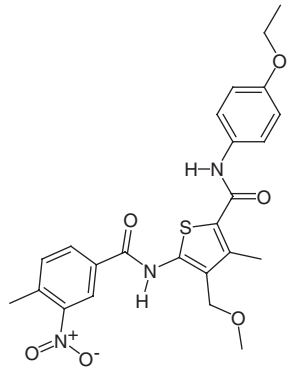	Nonmutagen	-0.020
ASN 11105444	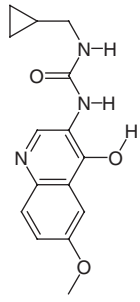	Nonmutagen	-3.62

score for the molecules and the molecules having positive values are considered to be mutagen, while, molecules with negative values are predicted to be nonmutagen. All the final hits were found to be nonmutagen (Table 4).

Conclusion

Kinase inhibitors still remain the most relevant drug molecules in lung cancer chemotherapy. Current research in NSCLC focuses on targeting T790M EGFR resistant tumors. Thus, in our present work, the dataset used covers a large applicability domain with wide activity range and diverse structures, thus this may have led to a putative broad-spectrum pharmacophore for EGFR (T790M) and cMET inhibitors. To determine the presence of crucial interactions with conserved amino acid residues in the active site, docking analysis was carried out. Finally, to validate the results obtained from docking and to study the stability molecular dynamic simulations were performed. Finally, the hits were found to be unreported as T790M EGFR and cMET, dual inhibitors for NSCLC. Thus, using a combination of various *in silico* techniques, we successfully identified three putative novel EGFR (T790M) and cMET inhibitors, which can be further evaluated by biological studies.

Future perspective

This research work done by the authors focus on the current issue of resistance in lung cancer, which is critical for lung cancer patients. This work is among the initial steps taken by researchers throughout the globe to target resistant lung cancer and the results of this work can be carry forwarded to the next stages of drug design and discovery. The final hits screened out could provide an eventual lead for the design and development of a dual inhibitor for lung cancer which is effective against resistant tumors. Also, the approach utilized in this work can be followed to design studies for countering other resistant targets or disease conditions.

Executive summary

Background

- Lung cancer, one of the prevalent forms of cancer, with around 1.35 million patients per year.
- It also remains the reason for high rate of cancer-related mortality worldwide.
- Non-small-cell lung cancer (NSCLC) form almost 85% of the total lung cancer cases.
- Patients with L858R mutation in EGFR, show positive response toward first-generation reversible tyrosine kinase inhibitors.
- T790M secondary mutation causes resistance toward first-generation tyrosine kinase inhibitors.
- Significant toxicities are observed with these second-generation inhibitors.
- There is another cross-talk mechanism, that is, amplification of cMET.
- Around 70% of NSCLC cases also show overexpression of cMET.
- Direct interaction between EGFR and cMET makes them simultaneously targetable.
- It is imperative to design molecule/s which can inhibit EGFR with T790M, along with cMET.

Materials & methods

- A total of 109 EGFR (T790M) and 90 cMET inhibitors were obtained from the literature.
- A total of 16 compounds for EGFR (T790M) and 19 compounds for cMET were randomly chosen as training set compounds.
- HypoGen-based pharmacophore models were built employing Discovery Studio 4.1.
- CDOCKER was used to execute molecular docking studies.
- Molecular dynamics simulations were run on computer terminal using Desmond.
- In pharmacophore generation process, for the EGFR (T790M) and cMET inhibitors, the uncertainty value was kept 3.
- The pharmacophore mapping features were assigned values from a range of 0–5 with the minimum inter-feature distance of 3.5 Å.
- Out of the 10 models, the most optimum model was chosen based on correlation value, test set prediction and cost analysis.
- Pharmacophore models were validated by methods such as EF and GH score, Fischer's randomization test and ROC curve.
- Databases namely, Asinex, Chembridge and Maybridge, were screened by EGFR (T790M) and cMET pharmacophore models.
- Protein crystal structure of EGFR (T790M) (PDB: 3W2P) and cMET (PDB: 3DKF), respectively, were extracted from Protein Data Bank.
- Docked molecules were forwarded for the molecular dynamics simulations using OPLS_2005 forcefield based Desmond software.

Result & discussion

- The pharmacophore hypothesis for EGFR, $EGFR4_{ADDH}$ consisted of four features: hydrogen bond acceptor, two hydrogen bond donor and hydrophobic.
- For cMET, $cMET1_{DHHR}$ consisted of four features: hydrogen bond donor, two hydrophobic and ring aromatic.
- Both the models, $EGFR4_{ADDH}$ and $cMET1_{DHHR}$ were validated using methods mentioned in materials and methods.
- Both $EGFR4_{ADDH}$ and $cMET1_{DHHR}$ showed values of all the validation parameters in the acceptable range.
- Docking of hits from cross-screening against both EGFR (T790M) and cMET was performed.
- After visual examination, 275 compounds showing key interactions were selected.
- Clustering on the basis of structural features, which yielded 11 molecules.
- A total of 22 complexes, with both EGFR (T790M) and cMET proteins, were exposed to MD simulations for a time frame of 10 ns.
- Careful investigation of simulation-interaction diagrams revealed overall three molecules to retain the conserved interactions in both the proteins.
- Finally, MM-GBSA method showed the binding energy value of -90.69 kcal/mol for EGFR (T790) best-hit complex and -72.26 kcal/mol for cMET best-hit complex.

Conclusion

- The hits were found to be unreported as T790M EGFR and cMET, dual inhibitors for NSCLC.
- Thus, using a combination of various *in silico* techniques, we successfully identified three putative novel EGFR (T790M) and cMET inhibitors.

Author contributions

PK Singh performed the study and wrote the paper; O Silakari supervised the project.

Financial & competing interests disclosure

The authors thank the Department of Biotechnology (DBT), New Delhi for awarding funds and junior research fellowship (JRF); BT/PR8275/BID/7/455/2013. The authors have no other relevant affiliations or financial involvement with any organization or entity with a financial interest in or financial conflict with the subject matter or materials discussed in the manuscript apart from those disclosed.

No writing assistance was utilized in the production of this manuscript.

Availability of data and materials

The authors wish to share the data used in this study. Please contact the corresponding author for more information.

References

Papers of special note have been highlighted as:
• of interest; •• of considerable interest

1 Walter AO, Sjin RTT, Haringsma HJ *et al.* Discovery of a mutant-selective covalent inhibitor of EGFR that overcomes T790M-mediated resistance in NSCLC. *Cancer Discov.* 3(12), 1404–1415 (2013).

2 Molina JR, Yang P, Cassivi SD, Schild SE, Adjei AA. Non-small-cell lung cancer: epidemiology, risk factors, treatment, and survivorship. *Mayo Clin. Proc.* 83(5), 584–594 (2008).

3 Rosell R, Carcereny E, Gervais R *et al.* Erlotinib versus standard chemotherapy as first-line treatment for European patients with advanced EGFR mutation-positive non-small-cell lung cancer (EURTAC): a multicentre, open-label, randomised Phase III trial. *Lancet Oncol.* 13(3), 239–246 (2012).

4 Helena AY, Arcila ME, Rekhtman N *et al.* Analysis of tumor specimens at the time of acquired resistance to EGFR-TKI therapy in 155 patients with EGFR-mutant lung cancers. *Clin. Cancer. Res.* 19(8), 2240–2247 (2013).

5 Yun C-H, Mengwasser KE, Toms AV *et al.* The T790M mutation in EGFR kinase causes drug resistance by increasing the affinity for ATP. *Proc. Natl Acad. Sci. USA* 105(6), 2070–2075 (2008).

• **The authors used the data presented by Yun *et al.* about the mechanism of resistance development against first-generation inhibitors in case of secondary-acquired mutant T790M EGFR, in lung cancer. They reported the interesting hypothesis which explains the actual reason, that is, increase in affinity for natural substrate ATP in case of T790M EGFR rather than presumed reason, that is, steric hindrance.**

6 Miller VA, Hirsh V, Cadranel J *et al.* Afatinib versus placebo for patients with advanced, metastatic non-small-cell lung cancer after failure of erlotinib, gefitinib, or both, and one or two lines of chemotherapy (LUX-Lung 1): a Phase IIb/III randomised trial. *Lancet Oncol.* 13(5), 528–538 (2012).

• **The authors followed the work of Miller *et al.* to understand the applicability of second-generation inhibitors, that is, covalent inhibitors. The work showed that though second-generation inhibitors are effective against resistant EGFR T790M lung cancer, they lack selectivity and thus possess high toxicity toward wild-type EGFR.**

7 Rong S, Bodescot M, Blair D *et al.* Tumorigenicity of the met proto-oncogene and the gene for hepatocyte growth factor. *Mol. Cell. Biol.* 12(11), 5152–5158 (1992).

8 Stella MC, Comoglio PM. HGF: a multifunctional growth factor controlling cell scattering. *Int. J. Biochem. Cell Biol.* 31(12), 1357–1362 (1999).

9 Engelman JA, Zejnullahu K, Mitsudomi T *et al.* MET amplification leads to gefitinib resistance in lung cancer by activating ERBB3 signaling. *Science* 316(5827), 1039–1043 (2007).

10 Bean J, Brennan C, Shih J-Y *et al.* MET amplification occurs with or without T790M mutations in EGFR mutant lung tumors with acquired resistance to gefitinib or erlotinib. *Proc. Natl Acad. Sci. USA* 104(52), 20932–20937 (2007).

11 Szklarczyk D, Franceschini A, Wyder S *et al.* STRING v10: protein–protein interaction networks, integrated over the tree of life. *Nucleic Acids Res.* 43, D447–D452 (2014).

•• **The researcher utilized the STRING online server reported by Szklarczyk *et al.*, to assess the protein–protein interactions between EGFR and cMET. These results obtained from server were utilized to design the study. As they reported a direct interaction between the two, thus, generating a possiblity of simulataneous inhibition of both.**

12 Boezio AA, Berry L, Albrecht BK *et al.* Discovery and optimization of potent and selective triazolopyridazine series of c-Met inhibitors. *Bioorg. Med. Chem. Lett.* 19(22), 6307–6312 (2009).

• **The authors included the data reported by Boezio *et al.*, in our study. The group reported a series of molecules which were significantly active as cMET inhibitors. The authors utilized the molecules reported by the group along with their IC_{50} value.**

13 Claridge S, Raeppel F, Granger M-C *et al.* Discovery of a novel and potent series of thieno [3, 2-b] pyridine-based inhibitors of c-Met and VEGFR2 tyrosine kinases. *Bioorg. Med. Chem. Lett.* 18(9), 2793–2798 (2008).

14 Porter J, Lumb S, Lecomte F *et al.* Discovery of a novel series of quinoxalines as inhibitors of c-Met kinase. *Bioorg. Med. Chem. Lett.* 19(2), 397–400 (2009).

15 Raeppel S, Claridge S, Saavedra O *et al.* N-(3-fluoro-4-(2-arylthieno [3, 2-b] pyridin-7-yloxy) phenyl)-2-oxo-3-phenylimidazolidine-1-carboxamides: a novel series of dual c-Met/VEGFR2 receptor tyrosine kinase inhibitors. *Bioorg. Med. Chem. Lett.* 19(5), 1323–1328 (2009).

16 Porter J, Lumb S, Franklin RJ *et al.* Discovery of 4-azaindoles as novel inhibitors of c-Met kinase. *Bioorg. Med. Chem. Lett.* 19(10), 2780–2784 (2009).

17 Mannion M, Raeppel S, Claridge S *et al. N*-(4-(6, 7-disubstituted-quinolin-4-yloxy)-3-fluorophenyl)-2-oxo-3-

phenylimidazolidine-1-carboxamides: a novel series of dual c-Met/VEGFR2 receptor tyrosine kinase inhibitors. *Bioorg. Med. Chem. Lett.* 19(23), 6552–6556 (2009).

18 Albrecht BK, Harmange J-C, Bauer D *et al.* Discovery and optimization of triazolopyridazines as potent and selective inhibitors of the c-Met Kinase. *J. Med. Chem.* 51(10), 2879–2882 (2008).

19 Cui JJ, Tran-Dubé M, Shen H *et al.* Structure based drug design of crizotinib (PF-02341066), a potent and selective dual inhibitor of mesenchymal–epithelial transition factor (c-MET) kinase and anaplastic lymphoma kinase (ALK). *J. Med. Chem.* 54(18), 6342–6363 (2011).

20 Norman MH, Liu L, Lee M *et al.* Structure-based design of novel class II c-Met inhibitors: 1. Identification of pyrazolone-based derivatives. *J. Med. Chem.* 55(5), 1858–1867 (2012).

- **The authors included the data reported by Norman *et al.*, in our study. The group reported a series of pyrazolone-based molecules which were significantly active as cMET inhibitors. The authors utilized the molecules reported by the group along with their IC_{50} value.**

21 Schroeder GM, An Y, Cai Z-W *et al.* Discovery of *N*-(4-(2-amino-3-chloropyridin-4-yloxy)-3-fluorophenyl)-4-ethoxy-1-(4-fluorophenyl)-2-oxo-1, 2-dihydropyridine-3-carboxamide (BMS-777607), a selective and orally efficacious inhibitor of the Met kinase superfamily. *J. Med. Chem.* 52(5), 1251–1254 (2009).

22 Garuti L, Roberti M, Bottegoni G. Irreversible protein kinase inhibitors. *Curr. Med. Chem.* 18(20), 2981–2994 (2011).

23 Liu LT, Yuan T-T, Liu H-H, Chen S-F, Wu Y-T. Synthesis and biological evaluation of substituted 6-alkynyl-4-anilinoquinazoline derivatives as potent EGFR inhibitors. *Bioorg. Med. Chem. Lett.* 17(22), 6373–6377 (2007).

- **The authors included the data reported by Liu *et al.* in our study. The group reported a series of quinazoline-based molecules which were significantly active against T790M-resistant EGFR. The authors utilized the molecules reported by the group along with their IC_{50} value.**

24 Pannala M, Kher S, Wilson N *et al.* Synthesis and structure-activity relationship of 4-(2-aryl-cyclopropylamino)-quinoline-3-carbonitriles as EGFR tyrosine kinase inhibitors. *Bioorg. Med. Chem. Lett.* 17(21), 5978–5982 (2007).

25 Smaill JB, Palmer BD, Rewcastle GW *et al.* Tyrosine kinase inhibitors. 15. 4-(phenylamino) quinazoline and 4-(phenylamino) pyrido [d] pyrimidine acrylamides as irreversible inhibitors of the ATP binding site of the epidermal growth factor receptor. *J. Med. Chem.* 42(10), 1803–1815 (1999).

26 Wissner A, Berger DM, Boschelli DH *et al.* 4-Anilino-6, 7-dialkoxyquinoline-3-carbonitrile inhibitors of epidermal growth factor receptor kinase and their bioisosteric relationship to the 4-anilino-6, 7-dialkoxyquinazoline inhibitors. *J. Med. Chem.* 43(17), 3244–3256 (2000).

27 Tsou H-R, Mamuya N, Johnson BD *et al.* 6-Substituted-4-(3-bromophenylamino) quinazolines as putative irreversible inhibitors of the epidermal growth factor receptor (EGFR) and human epidermal growth factor receptor (HER-2) tyrosine kinases with enhanced antitumor activity. *J. Med. Chem.* 44(17), 2719–2734 (2001).

28 Smaill JB, Showalter HH, Zhou H *et al.* Tyrosine kinase inhibitors. 18. 6-Substituted 4-anilinoquinazolines and 4-anilinopyrido [3, 4-d] pyrimidines as soluble, irreversible inhibitors of the epidermal growth factor receptor. *J. Med. Chem.* 44(3), 429–440 (2001).

29 Tsou H-R, Overbeek-Klumpers EG, Hallett WA *et al.* Optimization of 6, 7-disubstituted-4-(arylamino) quinoline-3-carbonitriles as orally active, irreversible inhibitors of human epidermal growth factor receptor-2 kinase activity. *J. Med. Chem.* 48(4), 1107–1131 (2005).

30 Discovery Studio version 4.1, Accelrys Inc., CA, USA. www.accelrys.com

31 Wu G, Robertson DH, Brooks CL, Vieth M. Detailed analysis of grid-based molecular docking: a case study of CDOCKER-A CHARMm-based MD docking algorithm. *J. Comput. Chem.* 24(13), 1549–1562 (2003).

32 Shivakumar D, Williams J, Wu Y, Damm W, Shelley J, Sherman W. Prediction of absolute solvation free energies using molecular dynamics free energy perturbation and the OPLS force field. *J. Chem. Theory Comput.* 6(5), 1509–1519 (2010).

- **The authors followed Shivakumar *et al.*'s work on Optimized Potential for Liquid Simulations (OPLS) forcefield to determine the forcefield to be used for the molecular dynamic simulations. The group reported extensive work on how suitable the OPLS forcefield is for the molecular dynamic simulations, which inspired the researchers to utilize OPLS forcefield during the work.**

33 Li H, Sutter J, Hoffmann R. HypoGen: an automated system for generating 3D predictive pharmacophore models. *Pharmacophore Perception, Development, and use in Drug Design (Volume 2)*. Internat'l University Line, CA, USA, 171 (2000).

34 Tai W, Lu T, Yuan H *et al.* Pharmacophore modeling and virtual screening studies to identify new c-Met inhibitors. *J. Mol. Model.* 18(7), 3087–3100 (2012).

- **The work from Tai *et al.* was followed by the authors to utilize the concept of receiving operating curve for the validation of the pharmacophore models. The paper provides a simple and exhaustive method of applying the receiving operating curve method to validate the ligand-based pharmacophore models.**

35 Guo Z, Mohanty U, Noehre J, Sawyer TK, Sherman W, Krilov G. Probing the α-helical structural stability of stapled p53 peptides: molecular dynamics simulations and analysis. *Chem. Biol. Drug Des.* 75(4), 348–359 (2010).

For reprint orders, please contact reprints@future-science.com

Therapeutic Delivery

The advantages of pulmonary delivery of therapeutic siRNA

"Pulmonary delivery of therapeutic siRNA provides a promising therapeutic modality for the treatment of numerous lung diseases."

Keywords: gene therapy • inhalation • nanoparticle • pulmonary delivery • siRNA

Pulmonary delivery of drugs has been an increasingly attractive area of research. The pulmonary route provides the possibility of noninvasive administration of pharmaceuticals to the local area along with administering to the systemic circulation [1]. There are a number of diseases that can be targeted via the local administration such as asthma, chronic obstructive pulmonary disease, microbial infections, cystic fibrosis, emphysema and lung cancer [2]. Targeting the systemic circulation is also possible as the lungs provide several features that are favorable for drug absorption, for example, large surface area, ultra thin epithelium, low enzymatic activity and a rich blood supply [3]. The US FDA approved the first formulation of inhaled insulin in 2006 which exhibits the potential for pulmonary delivery of drugs to provide treatment of systemic diseases [4]. There are several ways to deliver drugs to the lung. In animal models, these include administration through inhalation, intranasal and intratracheal routes. However, in human patients, intratracheal administration is less practicable. In fact, inhalation is the most common method for pulmonary delivery of drugs but requires formulations of liquid aerosol or dry powder [5]. Intranasal administration is another common route and benefits from the ease of administering nasal suspensions. One downside of intranasal administration is the difference in anatomical structures of the nose versus the lung, such as the narrower airway lumen that results in loss of drug concentration reaching the lung [6]. The intratracheal route is mainly employed for pulmonary delivery experimental set-ups and requires that the drug be instilled into the trachea. Due to the relatively invasive and nonphysiologic nature of this route of administration, the intratracheal route of pulmonary delivery is generally used in animal studies as a proof of concept model rather than clinical trials [7]. Regardless of the specific pulmonary administration route employed, pulmonary delivery has received increased attention due to its potential to successfully deliver protein and peptide drugs as well the promise of providing a mechanism for effective gene therapy delivery.

Gene therapy involves the use of nucleic acids to be formulated as drugs in an effort to treat diseases by replacing or interfering with a mutated, pathologically lacking or overexpressed gene of interest. One method of gene silencing therapy that has been widely studied involves the therapeutic delivery of exogenous double-stranded RNA that can be introduced into cells and processed by the enzyme Dicer to produce 21–23 nucleotide small interfering RNAs (siRNAs). These siRNAs are then able to guide silencing of target messenger RNA through base pairing mechanisms and through the multiprotein complex known as the RNA-induced silencing complex [8]. RNA interference through these siRNAs can be used to silence specific genes involved in the pathogenesis of various diseases associated with a known genetic background. Specifically, diseases and conditions that involve the epithelial layer of cells that make up the lining of the lungs are prime candidates for gene silencing through siRNA. Lethal lung disorders such as cystic fibrosis, pulmonary fibrosis, lung cancer and respiratory syncytial virus are all known to

Daniel P Feldmann
Department of Oncology, Wayne State University, Detroit, MI 48201, USA

Olivia M Merkel
Author for correspondence:
Department of Oncology, Wayne State University, Detroit, MI 48201, USA
and
Department of Pharmaceutical Sciences, Wayne State University, Detroit, MI 48201, USA
Tel.: +1 313 577 1523
Fax: +1 313 577 2033
olivia.merkel@wayne.edu

FUTURE SCIENCE part of fsg

be involved with the lung epithelium and would benefit from efficient therapies that target the mutated gene/s responsible for pathogenesis [9]. Over the last 4 years, a substantial amount of research has been published focusing on pulmonary RNA interference for the treatment of lung cancer. With lung cancer being the leading cause of cancer death, therapeutic siRNA could be a promising option for treatment that may reduce the systemic side effects seen with traditional chemotherapy while addressing the molecular root cause of the disease sequence specifically.

Although the application of siRNA to treat genetic diseases has a positive outlook, various barriers exist that must be overcome in order for the treatment to be effective. Traditional intravenous injections of siRNA have proven to have little ability to provide a therapeutic effect [10]. The cause for this stems from the fact that postadministration *in vivo*, the therapeutic siRNA must navigate the circulatory system of the body while avoiding kidney filtration, serum protein aggregation and enzymatic degradation by nucleases [11]. Delivery of therapeutic siRNA to the lung is an attractive option when considering these barriers. siRNA delivered to the lungs would reach the epithelium directly and thereby avoid any possible kidney filtration that may occur if it were injected intravenously. Contrary to oral formulations, pulmonary delivery of siRNA eliminates the first pass metabolism phenomenon due to the direct delivery of the therapeutic siRNA to the target tissue leading to a significantly higher concentration of drug exposure [12]. In turn, the close proximity of the therapeutic siRNA to the epithelial cells that play the biggest role in the majority of pulmonary disorders helps to dramatically increase the bioavailability of the siRNA while increasing the efficacy of the siRNA at lower doses. Consequently, this focused exposure of therapeutic siRNA through pulmonary administration will ultimately lead to reduced systemic side effects that would be seen with similar concentrations in plasma following intravenous or oral administration [13]. Due to the significantly reduced distance between the epithelial surface and blood found in the alveolar area (0.5 μm–1.0 μm), the siRNA that is deposited could be absorbed very quickly, which can increase the overall systemic siRNA drug action and allow for sufficiently high absorption of the siRNA [14]. Pulmonary delivery of siRNA also eliminates the possibility for serum protein aggregation that occurs when intravenous administration is performed due to the absence of serum within the air side of the lung. Once deposited within the lung, the therapeutic siRNA will also avoid nuclease degradation due to low levels of nuclease activity in comparison to those found within the systemic circulation [15].

While there are numerous advantages to pulmonary delivery of siRNA, there also exist several key barriers that must be considered. Comparatively, the typical siRNA duplex considered for therapeutic use weighs 13 kDa and has approximately 50 times the molecular mass of a small molecule drug that is well suited for absorption by the lung [16]. In addition, siRNA contains approximately 40 phosphates in its backbone resulting in an overall strong negative charge that contributes to poor uptake by the negatively-charged cell membrane. The lungs also possess intrinsic hurdles that must be addressed when considering pulmonary siRNA delivery. Due to the complex branched structure of the respiratory tract and the presence of surfactant coating the epithelial cells, efficient pulmonary delivery of siRNA takes place in the lower respiratory tract [17]. The lungs also exhibit active clearance processes such as mucociliary clearance and cough clearance that will serve to remove the siRNA once it has been administered [18]. There is also a high level of immune surveillance that is mediated through macrophages and polymorphic neutrophils which serve to prevent foreign material from entering into the lung. The presence of these clearance processes along with the transient nature inherent to RNA interference will facilitate the need for frequent siRNA administration in order to provide a therapeutic benefit. Despite these barriers, there have been reports of successful local siRNA therapy for the reduction of respiratory syncytial virus titers in the lung and protection from SARS infection after delivery of 'naked' siRNA [19].

In order to expand the use of pulmonary delivery of siRNA, it will be necessary to further develop carrier systems that will allow for an efficient therapeutic effect. To achieve this, both viral and nonviral delivery systems are being assessed. Viral vectors, such as adenoviruses and retroviruses have demonstrated the ability to mediate gene silencing in an *in vitro* lung model while lentivirus-mediated siRNA to nuclear protein 1 was able to inhibit tumor growth *in vivo* [20]. As an alternative to viral delivery systems, nonviral vectors, such as lipid and polymer-based vectors have shown great potential due to their reduced toxicity and immunogenicity. Positively-charged lipid-based carriers are easily formulated and achieve high transfection efficacy *in vitro* and *in vivo* due to their interaction with the negatively-charged cell membrane. Similarly, positively-charged polymers have been studied for their use in siRNA delivery to the lungs. Polymer-based vectors have the added benefit of being relatively nonimmunogenic and are able to withstand the process of aerosolization. Therefore, these polymer–siRNA complexes would be able to be delivered to the lungs through the inhalation route *via* a metered dose

inhaler or dry powder inhaler. Administration *via* these devices would ultimately improve rapid administration, ease of transportation and the stability of the drug formulation.

Pulmonary delivery of therapeutic siRNA provides a promising therapeutic modality for the treatment of numerous lung diseases. These pulmonary delivery applications are an attractive administration route for siRNA since they are noninvasive, biocompatible and have the possibility of being administered directly by the patient through aerosolization. With the recent advancement of pulmonary siRNA delivery to the clinic, it is more than probable that RNA interference-based therapy will be used in the future treatment of lung cancer. Nevertheless, further advances in delivery methods along with a more detailed understanding of gene silencing-based therapy will be required for these therapies to become a reality.

Financial & competing interests disclosure

The authors have no relevant affiliations or financial involvement with any organization or entity with a financial interest in or financial conflict with the subject matter or materials discussed in the manuscript. This includes employment, consultancies, honoraria, stock ownership or options, expert testimony, grants or patents received or pending, or royalties.

No writing assistance was utilized in the production of this manuscript.

References

1 Patil JS, Sarasija S. Pulmonary drug delivery strategies: a concise, systematic review. *Lung India* 29(1), 44–49 (2012).

2 Pison U, Welte T, Giersig M, Groneberg DA. Nanomedicine for respiratory diseases. *Eur. J. Pharmacol.* 533(1–3), 341–350 (2006).

3 Kleinstreuer C, Zhang Z, Donohue JF. Targeted drug-aerosol delivery in the human respiratory system. *Annu. Rev. Biomed. Eng.* 10, 195–220 (2008).

4 Ceglia L, Lau J, Pittas AG. Meta-analysis: efficacy and safety of inhaled insulin therapy in adults with diabetes mellitus. *Ann. Intern. Med.* 145(9), 665–675 (2006).

5 Lavorini F. The challenge of delivering therapeutic aerosols to asthma patients. *ISRN Allergy* 2013, 102418 (2013).

6 Groneberg DA, Witt C, Wagner U, Chung KF, Fischer A. Fundamentals of pulmonary drug delivery. *Respir. Med.* 97(4), 382–387 (2003).

7 Driscoll KE, Costa DL, Hatch G *et al.* Intratracheal instillation as an exposure technique for the evaluation of respiratory tract toxicity: uses and limitations. *Toxicol. Sci.* 55(1), 24–35 (2000).

8 Elbashir SM, Lendeckel W, Tuschl T. RNA interference is mediated by 21- and 22-nucleotide RNAs. *Genes Dev.* 15(2), 188–200 (2001).

9 Whitehead KA, Langer R, Anderson DG. Knocking down barriers: advances in siRNA delivery. *Nat. Rev. Drug Discov.* 8(2), 129–138 (2009).

10 Ryther RC, Flynt AS, Phillips JA, 3rd, Patton JG. siRNA therapeutics: big potential from small RNAs. *Gene Ther.* 12(1), 5–11 (2005).

11 Alexis F, Pridgen E, Molnar LK, Farokhzad OC. Factors affecting the clearance and biodistribution of polymeric nanoparticles. *Mol. Pharm.* 5(4), 505–515 (2008).

12 Carvalho TC, Carvalho SR, Mcconville JT. Formulations for pulmonary administration of anticancer agents to treat lung malignancies. *J. Aerosol. Med. Pulm. Drug Deliv.* 24(2), 61–80 (2011).

13 Vaughn JM, Mcconville JT, Burgess D *et al.* Single dose and multiple dose studies of itraconazole nanoparticles. *Eur. J. Pharm. Biopharm.* 63(2), 95–102 (2006).

14 Patton JS, Byron PR. Inhaling medicines: delivering drugs to the body through the lungs. *Nat. Rev. Drug Discov.* 6(1), 67–74 (2007).

15 Merkel OM, Rubinstein I, Kissel T. siRNA delivery to the lung: what's new? *Adv. Drug Deliv. Rev.* 75, 112–128 (2014).

16 Akhtar S, Benter IF. Nonviral delivery of synthetic siRNAs *in vivo*. *J. Clin. Invest.* 117(12), 3623–3632 (2007).

17 Sanders N, Rudolph C, Braeckmans K, De Smedt SC, Demeester J. Extracellular barriers in respiratory gene therapy. *Adv. Drug Deliv. Rev.* 61(2), 115–127 (2009).

18 Lebhardt T, Roesler S, Beck-Broichsitter M, Kissel T. Polymeric nanocarriers for drug delivery to the lung. *J. Drug Deliv. Sci. Technol.* 20(3), 171–180 (2010).

19 Merkel OM, Kissel T. Nonviral pulmonary delivery of siRNA. *Acc. Chem. Res.* 45(7), 961–970 (2012).

20 Guo X, Wang W, Hu J *et al.* Lentivirus-mediated RNAi knockdown of NUPR1 inhibits human nonsmall cell lung cancer growth *in vitro* and *in vivo*. *Anat. Rec.* 295(12), 2114–2121 (2012).